CEAS Space Journal
https://doi.org/10.1007/s12567-026-00727-x

ORIGINAL PAPER

SpaceLiner: the 2025 pre-definition status report

Martin Sippel[1] · Steffen Callsen[1] · Sunayna Singh[1] · Jascha Wilken[1] · Leonid Bussler[1] · Silvia Rodriguez-Donaire[2] · Daniel Garcia-Almiñana[2]

Received: 12 December 2025 / Revised: 3 March 2026 / Accepted: 14 April 2026

Abstract
Work on the SpaceLiner ultra-high-speed rocket-propelled passenger transport is now the focus of Phase A conceptual design evolution, mainly addressing system aspects of the next configuration release 8. The second role of the SpaceLiner concept as a TSTO launch vehicle for space transport is retained, and in this context, suitable precursor steps are investigated. The SpaceLiner cabin integration is an important aspect to be addressed as well as the feasibility of performing multiple missions compliant with noise and sonic boom constraints. The passenger capsule's shape has been iterated by multidisciplinary design analyses aiming for aerodynamic stability in a wide range of flight conditions. The thermal protection system of both stages is adapted and is evaluated for the passenger stage for multiple missions. A worldwide network of point-to-point missions with minimized impact of sonic boom on the overflown population is assessed. The challenges of finding a passenger rescue capsule with improved aerodynamic stability in the full flight regime are summarized. Finally, the development roadmap is linked to key elements of potential future European reusable heavy-lift launchers as precursors to the SpaceLiner and an update of estimated costs is presented.

Keywords SpaceLiner · RLV · SLME · TPS · Trajectory optimization

Abbreviations

CAD	Computer-aided design
CFD	Computational fluid dynamics
CRS	Cabin rescue system
DOF	Degrees of freedom
GLOW	Gross lift-off mass
LH2	Liquid hydrogen
LOX	Liquid oxygen
MR	Mixture ratio
MRR	Mission requirements review
RCS	Reaction control system
RLV	Reusable launch vehicle
SLB	SpaceLiner booster stage
SLC	SpaceLiner cabin
SLME	SpaceLiner main engine
SLO	SpaceLiner orbiter stage
SLP	SpaceLiner passenger stage
SSME	Space shuttle main engine
TPS	Thermal protection system
TSTO	Two-stage-to-orbit
TVC	Thrust vector control
e.c.	Economic conditions

✉ Martin Sippel
Martin.Sippel@dlr.de

[1] Space Launcher Systems Analysis (SART), DLR, 28359 Bremen, Germany

[2] UPC -ETSEIAAT, Barcelona, Spain

1 Introduction

From the very beginning of the technical concept definition, a central premise of the SpaceLiner was its potential to enable sustainable and cost-effective space transportation into orbit, while simultaneously revolutionizing travel over extremely long distances between different points on Earth. The manufacturing and operating costs of reusable launch vehicles are expected to decrease drastically through continuous production and regular daily launches. Current routine operations of the SpaceX Falcon9 indicate the viability of this vision.

DLR's SpaceLiner concept is similar in certain aspects to the idea of multiple-mission reusable launch vehicles. These concepts make it possible to carry out diverse missions with the same or at least a similar vehicle. The most prominent example in this category is the SpaceX Starship and SuperHeavy [1, 27]. While in its primary role

Published online: 05 May 2026

it is conceived as an ultrafast intercontinental passenger transport, in its second role, the SpaceLiner is intended as an RLV capable of delivering heavy payloads into orbit. Simulations of the SpaceLiner 7 orbital cargo version prove that reentry loads stay within the constraints of the PAX-version which confirms feasibility of the multiple-mission intention.

First proposed in 2005 [2], the SpaceLiner is under constant development and descriptions of some major updates have been published since then [3, 5–8, 12, 13, 19, 20, 31, 32]. The European Union's 7th Research Framework Programme has supported several important aspects of multidisciplinary and multinational cooperation in the projects FAST20XX, CHATT, HIKARI, and HYPMOCES. In the EU's Horizon 2020 program, the project FALCon addressed the advanced return recovery mode "in-air-capturing" to be used by the reusable booster stage [15, 16]. The integration of hypersonic point-to-point transports like SpaceLiner in future controlled airspace was addressed in the SESAR-project ECHO. The SpaceLiner has been one of the reference concepts and its feasible intercontinental trajectories have been refined in dedicated analyses [15].

An important milestone was reached in 2016 with the successful completion of the Mission Requirements Review (MRR) which allows the concept to mature from research to structured development [12]. The Mission Requirements Document (MRD) [4] is the baseline and starting point for all technical and programmatic follow-on activities of the SpaceLiner Program.

Beyond the visionary technical concept, the SpaceLiner serves as a source of inspiration for artists and designers. A screenshot from the animation video is showing the launch sequence in Fig. 1.

Fig. 1 SpaceLiner launch in animated video (https://www.youtube.com/watch?v=sZYE7Bo4Elc)

2 Architecture and key components of SpaceLiner

The two SpaceLiner stages, the reusable booster and the orbiter or passenger stage, are arranged in parallel at lift-off; see, e.g., Refs. [12, 19, 31, 32] This architecture significantly reduces the overall length of the launcher using the high-performance propellant combination LOX-LH2 which has the well-known disadvantage of the low-density hydrogen. In a more conventional stage tandem architecture, the total length of the stack could easily exceed 140 m with the drawback of large bending moments caused by two wings in atmospheric flight. Similar aerodynamic loads are also generated by the current layout, but are now not to be transmitted through a long and slender fuselage, but are to be distributed via a three-point stage attachment structure.

The main dimensions of the current, consolidated 7–3 configuration reach a total length of 82.3 m, a maximum span (of the booster) of 36 m and a total height of both stages mounted together of approximately 22 m [19, 31, 32].

2.1 Main propulsion system

Staged combustion cycle rocket engines offer the best performance and hence offer a key advantage for fully reusable stages which are inherently heavier than expendable rockets. Due to this consideration, such a closed cycle with moderate 16 MPa chamber pressure has been selected as the baseline propulsion system right at the beginning of the project [2]. A full-flow staged combustion cycle with a fuel-rich preburner gas turbine driving the LH2-pump and an oxidizer-rich preburner gas turbine driving the LOX-pump is the preferred design solution for the SpaceLiner Main Engine (SLME). The ambitious full-flow cycle is already used by SpaceX for its Starship and SuperHeavy with the Raptor engine for which an independent DLR performance assessment confirms much published data [38]. This SpaceX concept is in some aspects a similar multiple-mission reusable launch vehicle as SpaceLiner intends to become [7]. The Raptor engine is influenced by its interplanetary mission and hence uses a different propellant combination LOX-LCH4 which might one day be produced in-situ on Mars. The advantage of the combination of liquid oxygen with liquid hydrogen is the significantly better mass specific impulse at the cost of reduced propellant density and more complex operations due to the 20 K temperature of liquid hydrogen.

The SpaceLiner 7 has a requirement of vacuum thrust up to 2350 kN and a sea-level thrust of 2100 kN for the

booster engine and 2400 kN and 2000 kN, respectively, for the passenger stage. These values correspond to the mixture ratio of 6.5 with a nominal operational MR range requirement from 6.5 to 5.5. The SpaceLiner 8 configuration, now under preliminary definition, keeps engine thrust at similar levels as for the SL7. These are sufficient for applications up to super-heavy-lift launchers (see potential other applications in Ref. [14]) and are compatible with European ground test infrastructure constraints.

The expansion ratios of the booster and passenger stage/orbiter SLME engines are adapted to their respective operating conditions, while the mass flow, turbomachinery, and combustion chamber are assumed to remain identical in the baseline configuration [14]. Table 1 gives an overview about major SLME engine operation data for the nominal MR range as obtained by cycle analyses [14]. Performance data are presented for the two different nozzle expansion ratios of the SpaceLiner: 33 and 59. The full pre-defined operational domain of the SLME is shown in Ref. [14] including extreme operating points.

In 2024, the Swiss company SoftInway and DLR jointly completed a de-risk study for ESA on the SLME-type rocket engine. Eight High-Level Requirements and 21 Engine System Level Requirements have been defined [14]. The commercial AxSTREAM® software tool for turbomachinery analyses has been implemented by SoftInway. The following turbomachinery components have been pre-designed: low-pressure fuel pump and turbine, high-pressure fuel pump and turbine and high-pressure oxidizer pump and turbine [14].

Figure 2 shows major components of the SLME and their integration with the combustion chamber injector head and the routing of the main lines. The line dimensions are adapted to mass-flow requirements of the cycle analyses in the full domain, and stress and deformations are calculated by FEM.

An alternative architecture of the oxygen-rich preburner power pack is likely attractive for FFSC engines because of a more compact layout and hence significant mass savings potential. A linear arrangement of the turbopump and annular burner on top of the main combustion chamber (as with SpaceX Raptor) is called V9 [14] and is planned for more sophisticated investigation for the SLME.

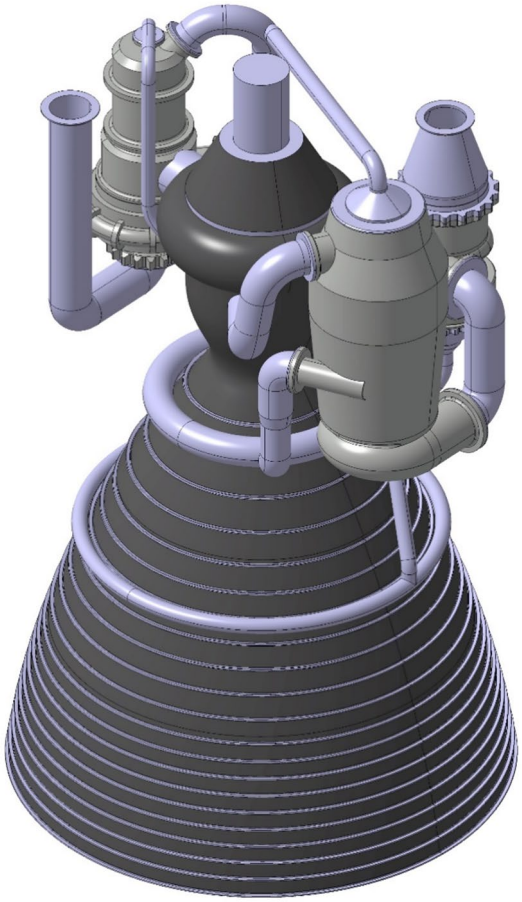

Fig. 2 SLME V7 with $\varepsilon = 33$ as a simplified CAD geometry showing arrangement of lines and turbomachinery [14]

The size of the SLME in the smaller booster configuration is a maximum diameter of 1800 mm and an overall length of 2982 mm. The larger passenger stage SLME has a maximum diameter of 2370 mm and an overall length of 3893 mm. The engine masses are estimated at 3500 kg with the large nozzle and at 3218 kg for the booster stage nozzle with an expansion ratio of 33. These values are equivalent

Table 1 SpaceLiner Main Engine (SLME) technical data from numerical cycle analysis [14]

Operation point	O1	O1	O2	O2	O3	O3
Mixture ratio [-]	6		6.5		5.5	
Chamber pressure [MPa]	16		16.95		15.1	
Mass flow rate in MCC [kg/s]	513.5		555		477.65	
Expansion ratio [-]	33	59	33	59	33	59
Specific impulse in vacuum [s]	436.9	448.95	433.39	445.97	439	450.56
Specific impulse at sea level [s]	385.9	357.77	386.13	361.5	384.2	352.6
Thrust in vacuum per engine [kN]	2200	2260.68	2358.8	2427.28	2056.7	2110.49
Thrust at sea level per engine [kN]	1943	1801.55	2101.6	1967.32	1800	1651.56

to vacuum T/W at MR = 6.0 of 65.9 and 69.7 [14]. Some optimization potential exists, mainly with the elimination of high-pressure LOX lines by introducing an advanced annular ox-rich powerhead of variant V9.

2.2 Reusable booster stage

The SpaceLiner (7) booster geometry is relatively conventional with two large integral tanks with separate bulkheads for LOX and LH2 which resemble the Space Shuttle External tank (ET) layout [6]. The major additions to the ET are an ogive nose for aerodynamic reasons and for housing subsystems, the propulsion system, and the wing structure with landing gear. The structure of the wing follows aircraft convention with ribs to make up the shape of the wing profile and spars to carry the main bending load [13]. Both tanks carry all major loads and the interface thrust to the upper stage is going through the intertank structure right in front of the LH2 tank. Engine thrust of 9 SLMEs and the ground support loads at the launch pad are directed through the conical thrust frame which is connected to the aft-Y-ring of the hydrogen tank.

The baseline recovery and return method of the reusable SpaceLiner booster stage is the patented "in-air-capturing" method which intends capturing and subsequently towing the winged vehicle using a sufficiently large subsonic aircraft. The procedure has been extensively investigated by increasingly refined simulations supported by lab-scale experiments demonstrating the high attractiveness in comparison with other recovery options (see Refs. [15–17]). Despite these promising results, the dry weight of the SLB at around 200 Mg [31, 32] puts a challenge on the availability of existing airliners having adequate towing capability. This critical point is under investigation and could influence the definition of SLB8.

2.3 Reusable upper stage

The SpaceLiner (7) fully reusable upper stage either carries the passengers to their destinations (then called SLP) or in a modified, unmanned version delivers cargo to orbit (SLO). In both versions, two SLME accelerate the vehicle from lift-off to its MECO. The aerodynamic shape is based on a single delta wing with moderate leading-edge radius which allows achieving (without flap deflection) an excellent hypersonic L/D of 3.5 at $M = 14$ assuming a fully turbulent boundary layer.

This achievement comes at the cost that in some areas of the SpaceLiner upper stage (leading edge and nose), the heat flux and temperatures exceed those values acceptable by CMC used in the passive TPS [5, 12]. Already early in the project, transpiration cooling using liquid water has been foreseen as a potential option for solving the problem [3, 9]. In the EU-funded project FAST20XX this innovative method has been experimentally tested in DLR's arc heated facility in Cologne using subscale probes of different porous ceramic materials [10]. Test results have been scaled to full size by heat transfer correlations and numerical assessment of the complete SpaceLiner trajectory [9]. Based on these data, a water storage tank system, a feedline manifold including control and check valves and some bypass and redundancy lines were preliminarily sized for accommodation inside the SpaceLiner volume for which an early mass estimation was obtained [11].

Besides the overall promising results, also some technical challenges of the active transpiration cooling system have been detected in the FAST20XX investigations [11, 20]. Therefore, the active transpiration cooling of leading edges and the nose is still the reference design option but could be replaced by other means of active cooling [11].

The SpaceLiner7 upper stage's internal design of the SLP has been adapted for its secondary role as an unmanned satellite launcher. The passenger cabin is not needed for this variant and is instead replaced by a large internal payload bay [12] as shown in Fig. 3. Key geometrical constraints and requirements are set so that the stage's outer mold line and aerodynamic configuration including all flaps should be kept unchanged for both variants. Though the internal arrangement of the vehicle could be adapted, a maximum commonality of internal components (e.g., structure, tanks, gear position, propulsion and feed system) is preferred because of cost reflections.

Further, the payload bay should provide sufficient volume for the accommodation of a large satellite and—if required—its orbital transfer stage. For this purpose, the SLO's propellant loading has been reduced by 24 Mg to 190 Mg compared to SLP with a smaller LOX-tank to allow for a payload bay length of 12.1 m and at least 4.75 m diameter [12]. These dimensions are close to the payload bay of the Space Shuttle (18.3 m × 5.18 m × 3.96 m) and should accommodate even super-heavy GTO satellites of more than 8 m in length and their respective storable upper stage [12]. Large doors open on the upper side to enable the easy and fast release of the satellite payload in orbit.

2.4 SpaceLiner Cabin and Rescue System

The passenger cabin of the SpaceLiner (SLC) has a double role. Providing first a comfortable pressurized travel compartment which allows for horizontal entrance of the passengers, the cabin in its second role serves as a reliable rescue system in case of catastrophic events. Thus, the primary requirements of the cabin are the possibility of being firmly attached late in the launch preparation process as well as a fast and safe separation in case of an emergency.

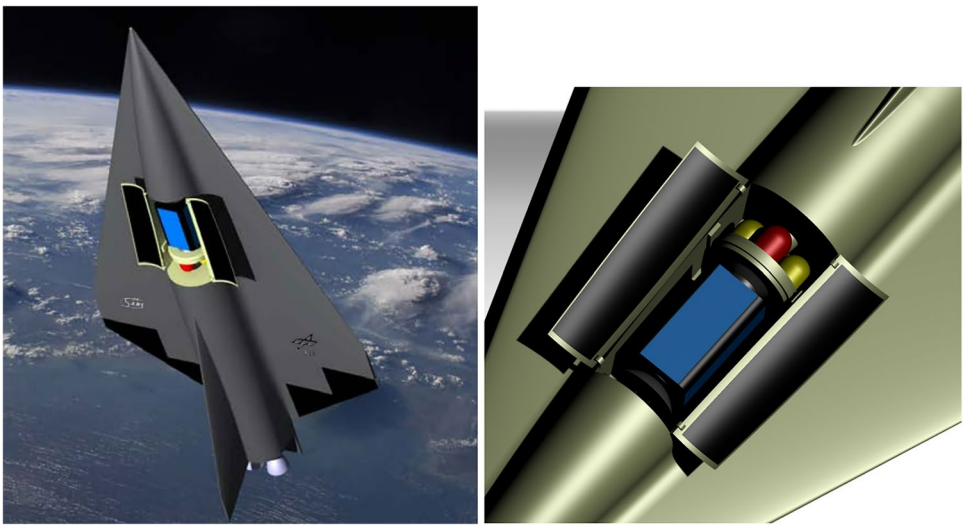

Fig. 3 SpaceLiner 7 orbital stage (SLO) in renderings with an open cargo bay and a payload with a kick-stage

The SpaceLiner MRD [4, 12] defines passenger safety requirements well beyond today's reliability of launch vehicles which are nevertheless indispensable to create a viable commercial product. A safety philosophy following a multiple-step approach is chosen [20] to address the MRD requirement.

The capsule's preliminary layout and its evolution are summarized in several publications, e.g., Refs. [5, 12, 13, 19, 20, 22, 24]. During nominal flight, the capsule in its baseline design is considered to have its upper part conformal with the topside of the passenger stage (SLP). The SLC lower section is clamped within the SLP without any load carrying structural connection (see, e.g., Ref. [13]) to allow rapid and safe separation in case of an emergency.

Five abort cases with SLC ejection along the nominal operational flight have been analyzed by multi-body simulations [19, 20, 24]. Initial conditions of the separation simulations have in all cases been selected from the nominal passenger flight trajectory without assuming any degradation in flight path or attitude due to anomalies. Obviously, this is a major simplification of potential emergency situations and does not reflect a worst-case scenario. However, the analyses presented in Refs. [19, 20] intended to use these trade-offs to serve in the definition of system requirements in the Phase A analyses.

A preliminary assessment of the simulation results in Refs. [19, 20] revealed that the lack of aerodynamic stability in a significant portion of the cabin's huge flight envelope develops into a problem because maximum acceptable acceleration loads on the passengers would be exceeded. The situation is relevant for the full section of SpaceLiner flight at elevated dynamic pressure. The SLC needs to be redesigned for SpaceLiner 8 so that its shape is aerodynamically stable or could rapidly morph into a stable configuration [20, 32]. Preliminary new design trade-offs are discussed in Sect. 3.5.

2.5 System masses

The SpaceLiner 7–3's GLOW reaches about 1832 Mg for the reference mission Australia–Europe, while the TSTO is at 1807 Mg still below that of the Space Shuttle STS of more than 2000 Mg. Tabulated data on the SL7 stages' dry and operational masses have been published in several previous papers; see, e.g., Refs. [31, 32].

3 Status of SpaceLiner 8

3.1 SL7 improvement potential

The biplane architecture of the mated launch configuration visible in Fig. 1 is problematic because of complex high-speed flow interactions of the two stages during ascent flight. A 6DOF-simulation based on simplified aerodynamics assuming perturbations and engine-out conditions indicates that the situation could probably be mastered by TVC [8, 13, 21]. Nevertheless, a less interacting, less complicated flow around the geometry of the ascent vehicle is desirable not least to avoid potential damage to surface insulation and coatings.

Both the complicated flow of the launch configuration and the shock–shock interaction during booster reentry [6, 13] have motivated the investigation of potential geometry changes and improvements to the SpaceLiner booster wing geometry. Attractive methods for the return of the booster stage are to be kept in mind. The challenge of towing the large and relatively heavy SLB by existing airliners (see previous Sect. 2.2) has an impact on the required subsonic aerodynamic quality if "in-air-capturing" is the preferred choice.

The integration of the passenger rescue system in the nose section of the upper stage and its reliable operation in all flight conditions is another critical aspect. Systematic

analyses of the separation process with the SLP7 design have been performed in selected critical flight points. A summary of these results is presented in Ref. [20] which highlights the necessity of a future redesign of the passenger stage (see also Sect. 2.4).

Currently, the study for the next SpaceLiner 8 design is still ongoing and it is too early to report a consolidated configuration. However, the latest results of preliminary analyses are presented in the following subsections.

3.2 Early iteration of SLB8 with small fixed wing

In order to reduce biplane flow interactions during ascent and to avoid the shock–shock interaction on the outboard leading edge, a drastically reduced size of the SLB wing had been investigated and a sketch of the concept was presented in Ref. [6]. The relatively small wing of the so-called SLB8V2 turns out to be fully sufficient for a smooth reentry avoiding extreme heat loads. However, the SLB8V2 would need to be designed for vertical downrange landing on a sea-going ship. The reentry could be somehow similar to SpaceX's Starship. After gliding deceleration to low speed and low altitude, the vehicle should rotate its attitude by 180 deg. and eventually some of the rocket engines are reignited for final slowing down to a vertical landing.

The turning maneuver of SLB8V2 with a fixed wing before its intended vertical landing was evaluated as a critical point for the feasibility of the concept due to the large propulsive moment required for a controlled pitch-turn maneuver [6]. Meanwhile, SpaceX has concluded several flight demonstrations with prototypes including atmospheric reentry. Starship is controlling its attitude by changing the dihedral deflection of both canard and main wing before performing the "belly-flop"-maneuver which rapidly brings the vehicle from almost horizontal into vertical orientation for landing. The turn is simply achieved by folding up the aft wing, and hence, eliminating lift and at low dynamic pressure, the TVC of three reignited SpaceX Raptor-engines controls attitude and decelerates the falling stage. Similar maneuvers were hardly achievable with the previously defined fixed-wing SLB8V2 as described in Ref. [6].

Although the successful flight tests of Starship can be understood as a major breakthrough, the innovative "sky-dive" and "belly-flop" maneuvers are highly demanding for the wing design and its control as well as the fast rocket engine reignition. Therefore, the suitability of this approach also for the safe and efficient operation of the SpaceLiner booster is still open for future evaluations.

Actually, the SuperHeavy first stage of SpaceX' Starship is closer in its role to the SpaceLiner Booster. However, this ultra-heavy launcher stage with lift-off masses in excess of 4000 Mg is designed for RTLS because any downrange landing would require outsize, non-existent ships as landing platform. Although, the SuperHeavy stage is making use of aerodynamic lift during hypersonic reentry, the toss-back maneuver and the vehicle capture in vertical flight require excessive amounts of propellants (DLR-analyses: > 260 t [27]). Therefore, the SpaceX approach is still deemed not attractive for future evolutions of the SpaceLiner Booster.

3.3 SLB8 option with swept wings

As the vertical landing SLB8V2 turned out to be not fully convincing, alternative designs have been explored [6, 8]. It has been tried to maintain the promising hypersonic aerodynamic configuration with small fixed wings. However, in order to support the stage to use "in-air-capturing" [15–17] and horizontal landing, deployable wing options have been checked on integration and mass impact [6, 8]. The challenge of this design is finding a suitable combination of different wing shapes which achieve a sufficiently high trimmed subsonic L/D of around 6, acceptable landing speed but also being fully trimmable in hypersonic flight at high angles of attack. A partially automatic variation of parameters was implemented in an MDA approach in order to systematically search for feasible and promising layouts [8]. The SLB8 V3 with deployable outer-wing option is shown in Fig. 4 in both aerodynamic configurations. Instead of trailing-edge flaps, the inner segment had separate spoilers on its lower and upper surfaces.

In the Iteration 3 of the SLB8 V3 design, it has been decided to add an additional 10th rocket engine to improve thrust-to-weight ratio at lift-off, thus, reducing gravity losses with an almost similar ascent propellant mass compared to SLB7-3. The fuselage diameter is increased to 8.8 m. As a consequence, the stage length reduces to 79.1 m. The span with the deployed outer segment reaches 53.8 m, while the span of the retracted wing is reduced to merely 28.8 m.

The cluster of 10 SLME when integrated in SLB8 V3 It. 3 (Fig. 5) can keep a distance of at least 2 m on the outer ring when measured from each engine's center axis which corresponds to a minimum distance at nozzle exit of approximately 250 mm [25]. The distance between the center engine and those on the outer ring is 3 m (comfortable 1200 mm at nozzle exit) [25]. The SLME-V9 variant with extended length would not exceed the SLB8 V3 bodyflap. However, the long bodyflap of V3 is driven by aerodynamic trim requirements of the vehicle and future SLB8 modifications might see a significantly shortened bodyflap.

3.3.1 Aerodynamic assessment

In the lower supersonic flight regime and in the subsonics, the SLB8 should be operated with the outer-wing segment fully deployed (Fig. 4, center). In an early assessment of the subsonic characteristics, empirical estimation methods

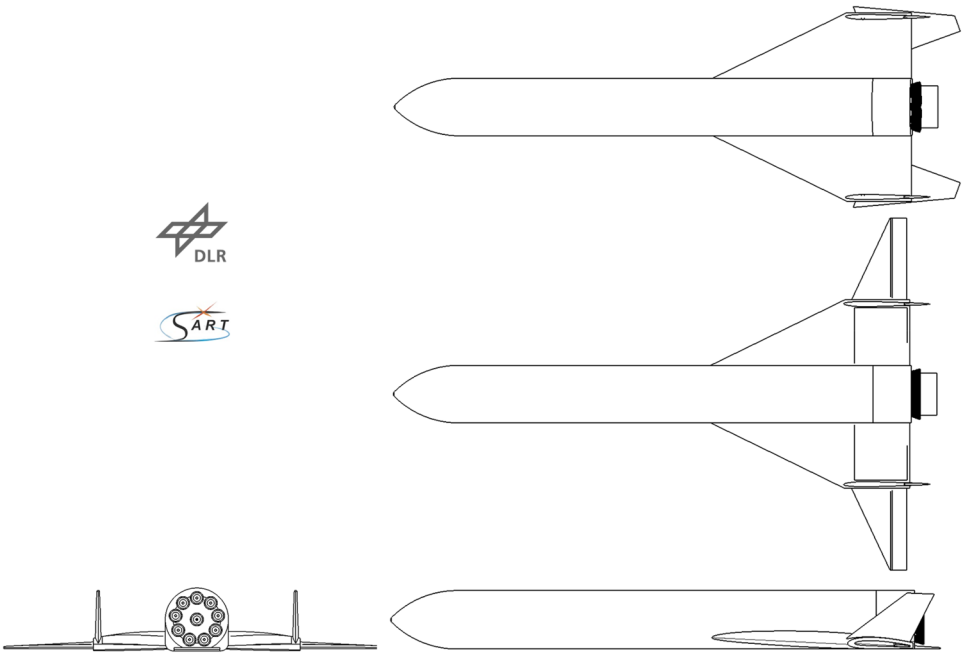

Fig. 4 Drawing of preliminary SLB8 variant V3 It. 3 with sweep-wing in stored (top) and deployed (center) position

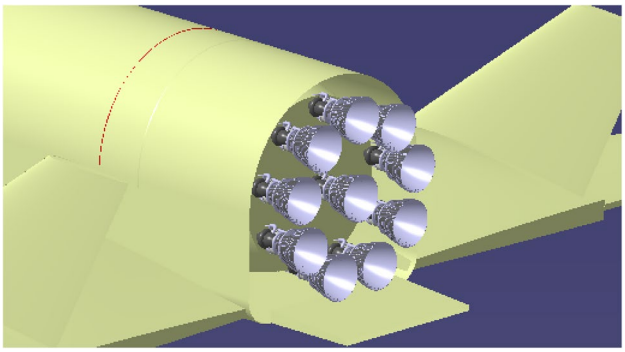

Fig. 5 CAD-view of 10 SLME-V9 integrated in base of SLB8 V3 [25]

have been used. Assuming the estimated CoG-position at the time of analyses [26], a negative (upward) spoiler deflection η of -11° on the main wing could reach a pre-trimmed state with the bodyflap neutral. The maximum L/D ratio might be around 6 at Mach numbers below 0.5 and an AoA of 10° (Fig. 6) based on engineering relations. At higher angles of attack, the wing might encounter flow separation and, hence, this region is to be avoided.

Pre-trim calculations based on the empirical aerodynamic methods should be treated with some caution. Therefore, the SLB8 V3 had been analyzed in subsonics at selected flight points also using the OpenFOAM (OF) tool under inviscid assumptions. In Refs. [26, 39], the obtained lift-to-drag ratios are compared to the empirically based calculation. The lift–curve slope is found very similar by both methods [26]. Under the circumstances of this preliminary analysis, the SLB8 V3 glide ratios at Mach 0.5 do not exceed 5.0 at the angles of attack of 10° and 14° [26, 39].

A significant positive spoiler and bodyflap deflection of around 10° and 20° would be required to reach roughly a trimmed state at elevated AoA in hypersonics as shown in Ref. [39]. Then, the configuration is neutral or marginally stable at best with some uncertainty on the actual pressure distribution due to a strong separated shock in front of the vehicle in case of high AoA-flight. The somehow sobering results demonstrate the challenge of achieving improved trimmed *L/D* in subsonic flight which, however, is essential for making the "in-air-capturing" recovery of the heavy RLV with empty weight above 200 tons feasible with existing aircraft. As this requirement is currently not fulfilled with the SLB7 [32], further improvements are to be investigated or alternative recovery solutions to be implemented. Trim behavior in hypersonics could be enhanced with a shorter fuselage of increased diameter. The SLB8 V3, nevertheless, is useful for evaluating integration of advanced TPS (see paragraph below) and testing different aerodynamic shapes. A converged SpaceLiner 8 booster is likely to have a significantly different shape to the one shown in Fig. 4.

3.3.2 Thermal protection assessment

A critical aspect for RLVs like the SpaceLiner is the selection of a reusable cryogenic tank insulation which works under multiple environmental conditions. Independent of weather conditions (e.g., temperature and humidity), effective insulation needs to be ensured and icing on the vehicle external surface is to be avoided. DLR has

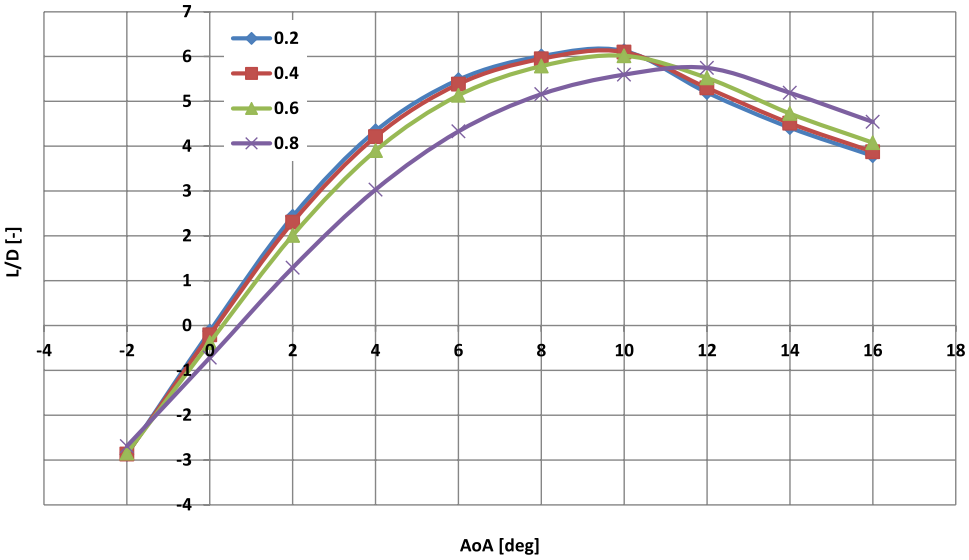

Fig. 6 Calculated trimmed, subsonic *L/D* ratios of SLB8 V3 with assumed negative spoiler deflection on the wing upper side [26]

performed systematic research on promising combinations of insulation and reentry TPS for which the SLB7-3 serves as the reference system concept. The booster stage's reusable cryogenic tank insulation has been investigated under consideration of the external TPS by numerical simulation and experiments [28, 30]. The preselected design option includes a so-called purge gap creating a distinct gap between the insulation of the cryogenic tank and the external thermal protection system [30], which has to be resistant to temperatures beyond typical limits of cryo-insulations. This relatively complex combination of external TPS and cryogenic insulation has been selected in order to avoid icing even in a humid and relatively cold environment [28]. In the gap, a forced flow of pre-heated dry gas is providing a controlled boundary condition at the outer interface of the cryogenic insulation. Results from the DLR projects AKIRA and TRANSIENT demonstrate the reusable insulation concept is functioning; however, a negative mass impact on the SLB stage is expected [30]. This effect is due to the increased weight per surface area but also by the reduced available volume for propellants inside the SLB because of the enlarged thermal protection thickness compared to the previous assumptions.

At the end of the AKIRA-project, such an influence on the reference system has been investigated using the SLB8 V3-variant presented in Ref. [8]. Three iteration steps were performed (see the short summary in Ref. [19]) considering the definition of the thermal protection system as well as cryogenic insulation based upon AKIRA investigations. A TPS with an external metallic surface (either Inconel or titanium or aluminum depending on the expected maximum temperatures) has been assumed.

The newly defined purge-gap TPS of the AKIRA-project has been applied to the SLB8 V3-variant. A TPS with external metallic surface (either Inconel or titanium or aluminum depending on the expected maximum temperatures) has been assumed. The preliminary TPS-type distribution of SLB8 is shown in Fig. 7. Almost the complete fuselage is protected by the metallic TPS with gap. The only exception is the nose cone which is a separate structure ahead of the forward LOX-tank dome. The wing, fin, spoiler and flaps have a more classical TPS layout. The upper side of the wing could be sized as a metallic hot structure with large areas not requiring insulation. The lower side of the wing and in particular the deflected spoiler and bodyflap experience most of the heat loads and could reach temperatures close to 2000 K for short periods. Ceramic materials are to be selected. In case of the spoiler and bodyflap, probably no major insulation layer will be required and instead a hot-structure CMC supported by steel frames on the leeward side could be the solution. Detailed investigations of this concept have not yet been performed.

3.3.3 Vehicle dry and lift-off mass

The estimated dry mass of the SLB8 V3 Iteration 3 had been estimated in 2020 at 220 Mg, roughly 10% more than SLB7-3 [26, 39]. Based on available subsystem sizing and empirical mass estimation relationships and the previously described preliminary TPS sizing, the stage masses have been reiterated to the slightly lower values listed in Table 2. The variable-sweep outboard wing and its mechanisms are a major uncertainty in the mass estimation.

The need for further dry mass reduction is obvious. Several options are to be explored in the next steps including

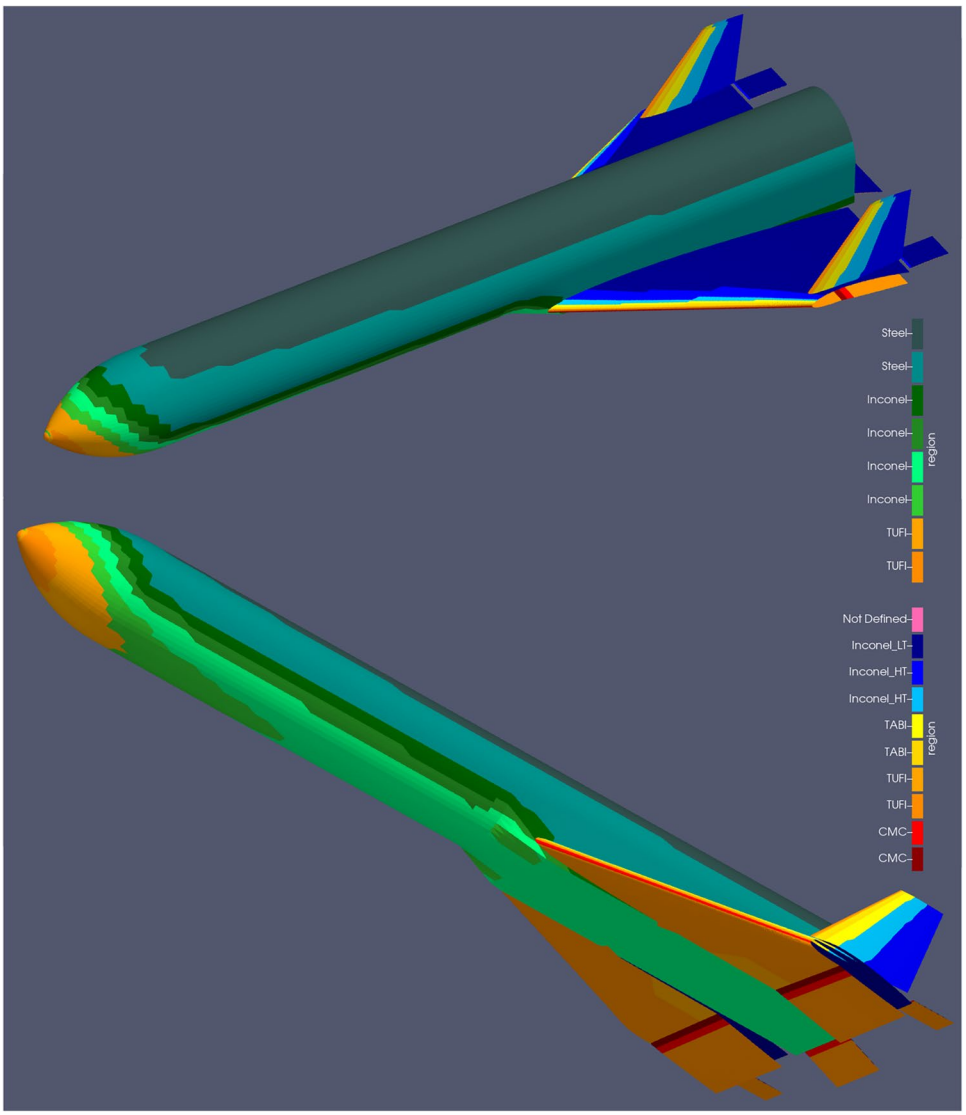

Fig. 7 TPS-type distribution on SLB8 V3 in views of the top and bottom sides

Table 2 Mass data of SpaceLiner 8 booster stage SLB8 V3 Iteration 3

Structure [Mg]	Propulsion [Mg]	Subsystem [Mg]	TPS [Mg]	Total dry [Mg]	Total propellant loading [Mg]	GLOW [Mg]
132.1	41.7	20.4	20.9	215	1281.6	1496.7

adapting the wing size, replacing the relatively heavy metallic surface TPS or adopting a more compact layout of the engine bay, inspired by the SpaceX Starship–SuperHeavy configuration.

3.4 SLP8 variant O40-0042

The upper stage has been subjected to an intensive shape variation and optimization process of the wing described in detail in Refs. [33–35]. The fuselage of the preliminary variant O40-0042 (Fig. 8) remains unchanged to SLP7, while the wing span and its overall surface have been significantly reduced. A future adaptation also of the fuselage is likely but requires as a first step the selection of a promising new design of the passenger capsule (SLC) [20, 32]. Recent results of ongoing systematic investigations for improving the aerodynamic characteristics of the SLC are reported in Ref. [37] and Sect. 3.5.

The more radical changes of the SLC as explained in Sect. 3.5 and Ref. [37] are not compatible with the SLP7 fuselage and together with a potentially different tank layout will see another MDAO-loop in the future.

The challenge in designing the SLP8 passenger stage is to find an aerodynamic shape that enables both long-range

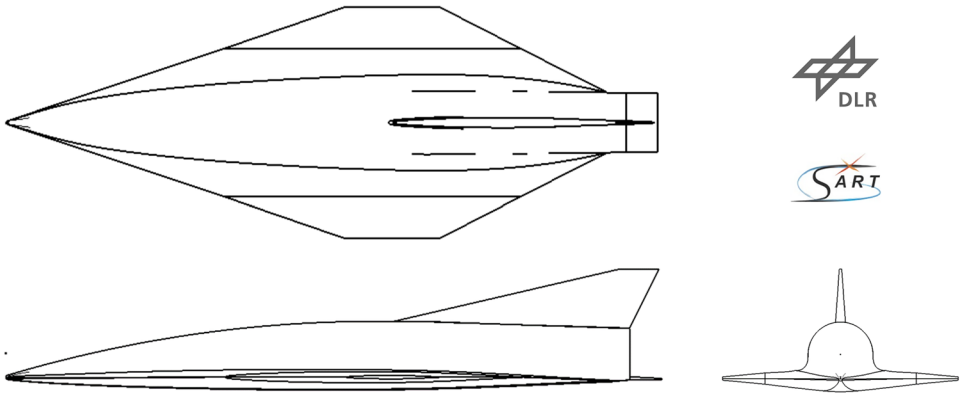

Fig. 8 Drawing of preliminary SLP8 variant O40-0042

glide flights with good hypersonic L/D, as in the case of SL7, and ballistic jumps outside the atmosphere over populated landmasses. For the latter, it is possible to drastically reduce noise on the ground (see the following paragraph on intercontinental trajectory options). However, then the configuration's design needs to generate increased lift by increased AoA during reentry to remain within acceptable heat loads.

To address these competing requirements, a systematic variation and optimization of potential design options for the SLP8 configuration was carried out in a multidisciplinary approach [32, 33]. Based on fast estimation methods, the geometry of the wings has been systematically varied with regard to maximum SLP hypersonic lift-to-drag ratio, maximum trimmable hypersonic lift generation as well as the resulting dry mass of the vehicle. In these analyses, other properties of the fuselage, such as the outer shape, the internal arrangement of tanks and engines and the large vertical stabilizer, are still kept similar to the SLP7. Future evolutions toward a consolidated SpaceLiner 8 configuration will be extended to modifications on these items as well.

The shift of the CoG induced by each geometry variation was preliminarily assessed and included in the generation of the pitch-trimmed aerodynamic datasets. In addition to pitch trim, other constraints such as a maximal permissible landing speed of 100 m/s and a feasible flight path through the entire velocity regime were considered. Finally, trajectory optimizations were used to evaluate the performance of the configurations on the Pareto front of the aerodynamic shape optimization [35].

Figure 9 shows a direct comparison between the wing planform of the preselected SLP8 variant O40-0042 obtained from the MDAO with respect to the SLP7. The major reduction in wing area is obvious. The SLP8 candidate has more forward-shifted wings, which provide better trim performance (improved relative position between the CoG and the hypersonic cop). In fact, this vehicle can generate more lift at hypersonic velocities than the SLP7 despite its smaller wings as it is trimmable up to at least 40° of angle of attack at reference Mach number 14 (while the SLP7 only up to 28°) [35].

3.4.1 Aerodynamic assessment

The SLP8 variant's aerodynamic performance in high-speed flight remains impressive despite the assumptions of reduced wing size but an untouched fuselage compared to SLP7. The maps of L/D ratios calculated with the surface inclination method in the very broad range of Mach numbers 4 to 28 and AoA from -4° to 44° are presented in Fig. 10 for two different cases. Following a typical flight profile, the boundary layer transition is assumed to occur below Mach 14 and 58 km while above the BL is assumed to stay mostly laminar. In the top position of Fig. 10, L/D of the clean configuration without deflections is depicted which might reach up to 5 at AoA below 10°. The trimmed state of this shape is reached between 10 and 12°. The supposed negative deflections of the data in the bottom plot are close to achieving longitudinally stable, trimmed conditions at angles of attack of around 40°.

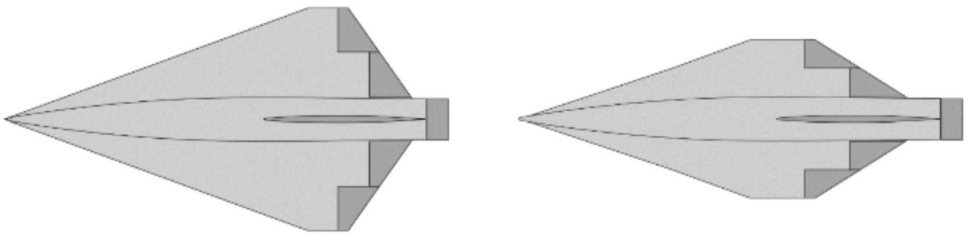

Fig. 9 Comparison between wing planform geometries of SLP7 (left) and SLP8 candidate O40-0042 (right) [35]

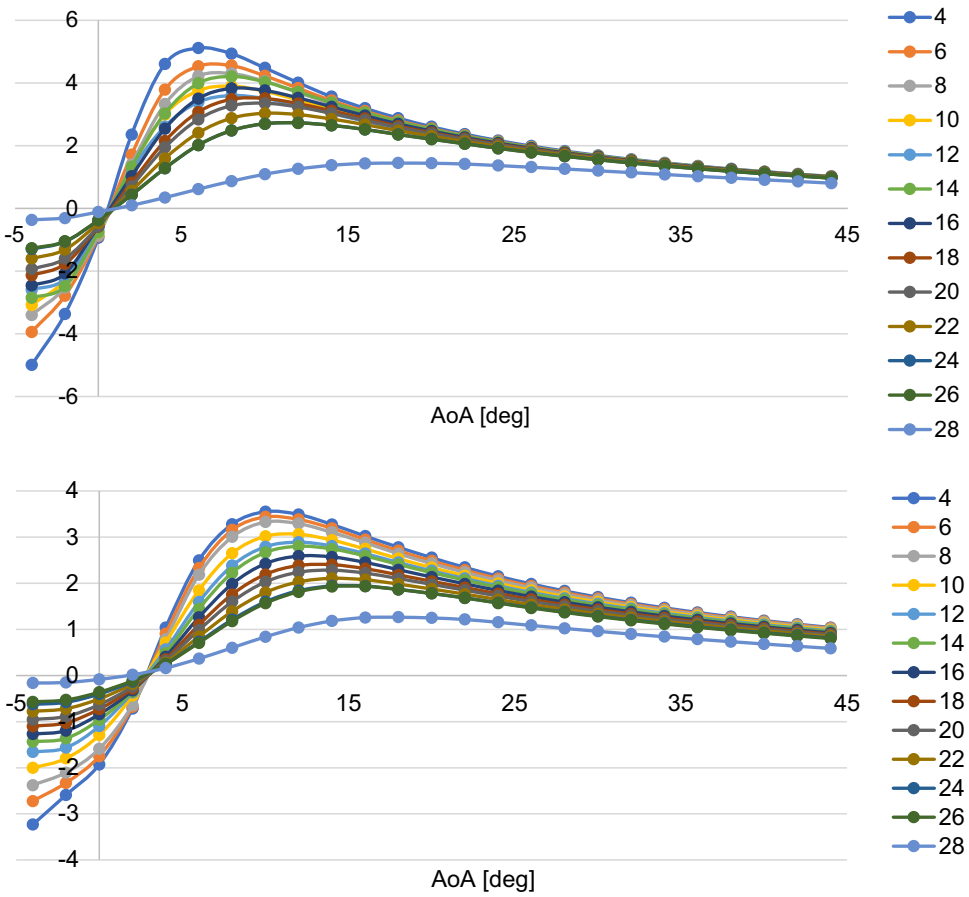

Fig. 10 Calculated hypersonic L/D ratio of SLP8 variant O40-0042, no deflections (top) and flap deflection angle $\eta = -20°$, BF deflection $-10°$ (bottom)

A comparison of the lift generation capabilities of these configurations shows a roughly fivefold increase of the trimmed c_L at 40° for SLP8 compared to typically 10° for SLP7.

The sensitivity of the aerodynamic characteristics to simplified modeling requires careful checks by CFD-(Euler-) methods before any configuration can be finally selected. In particular, the landing speed aerodynamics need to be considered to confirm the practical feasibility of the potentially smaller size wing. Inviscid Euler calculations with the OpenFOAM environment and the steady-state, compressible *rhoSimpleFoam* solver have been used. The hex-dominant meshes have been generated with the *snappyHexMesh* utility of OpenFOAM.

The subsonic flow condition of the SLP8 variant O40-0042 at a landing approach speed of Mach 0.3 is visualized in Fig. 11. A leading-edge vortex on the upper surface being typical for delta wings under such conditions is clearly visible. These vortices are responsible for the additional lift at high AoA conditions and have an important effect on surface pressure distribution and hence the pitch moment coefficient c_M.

The inviscid CFD data show non-linear behavior with increasing AoA due to vortex lift and indicate significantly higher c_L coefficients at AoA beyond 10° compared with results of the fast engineering methods used in the multidisciplinary design optimization. Therefore, the feasibility of the reduced size wing compared to SL7 is confirmed or might offer additional margins, even if viscosity effects may slightly reduce the calculated lift coefficient slope. A trimmed landing condition is reached with trailing-edge flaps deflected by 10° and speed slightly below 100 m/s. The SLP8 variant O40-0042 is longitudinally unstable under the current estimation of its likely CoG-position.

3.4.2 Thermal protection assessment

The external thermal protection has been preliminarily defined for the SLP8 following the SL7 pre-selection (e.g., Refs. [5, 12]). Figure 12 shows the stagnation point heat load along the flight duration for different point-to-point trajectories of SpaceLiner 8. Upon assessment, the Australia–Florida (USA) trajectory was identified as having the highest heat load and was therefore selected as the worst-case scenario for TPS sizing. In contrast, the Shanghai–California trajectory exhibits the lowest heat load and is analyzed to assess the sensitivity of the TPS sizing and mass.

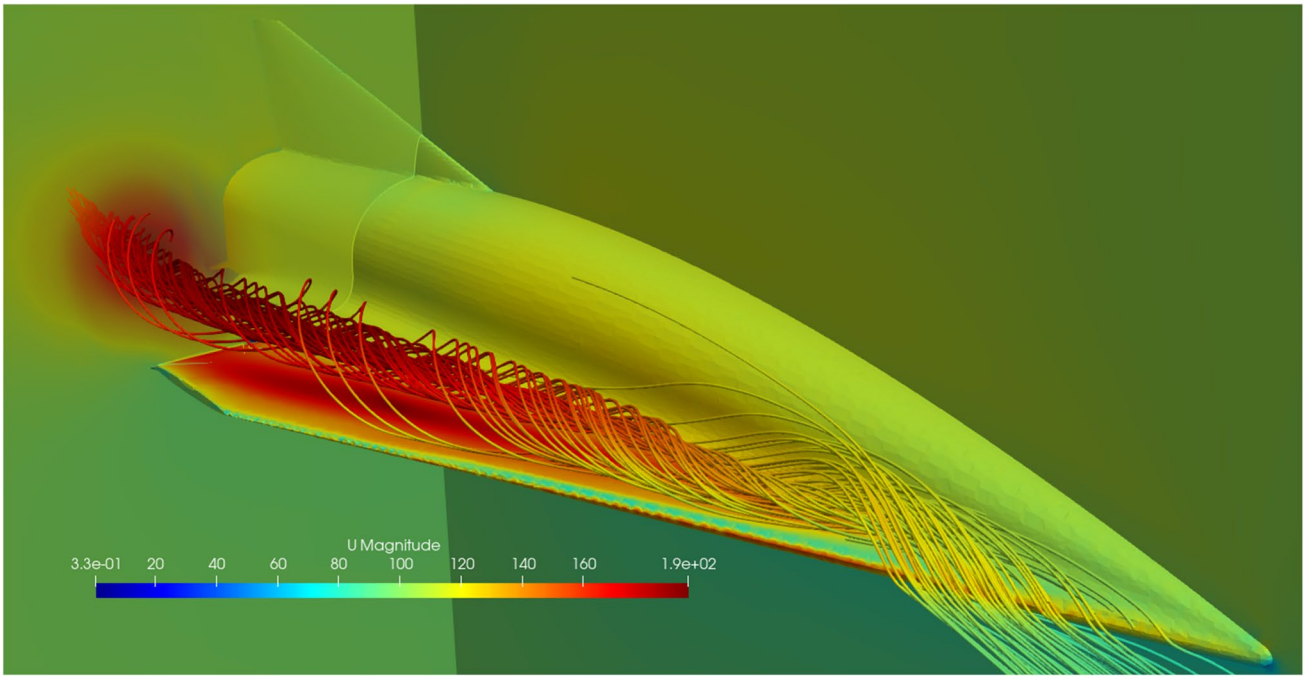

Fig. 11 Computed flow field on SLP8 variant O40-0042 in subsonics close to landing conditions ($M = 0.3$/AoA = 20°)

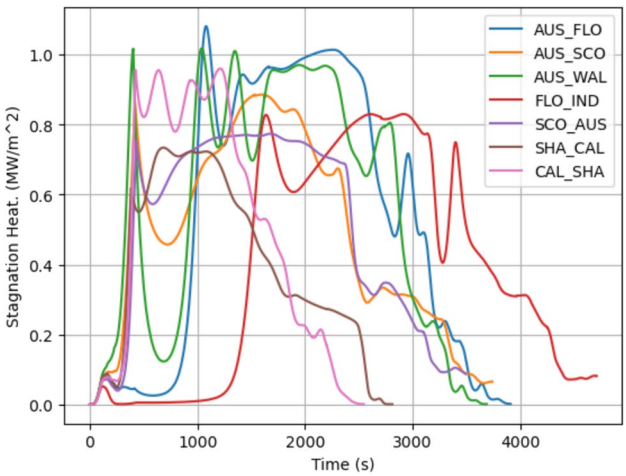

Fig. 12 Overview of stagnation heat for SpaceLiner 8 for different trajectory options

Figure 13 shows the TPS distribution on the upper and lower surfaces based on the selected SL8 worst-case reference trajectory (AUS_FLO). The TPS is expected to endure the loads of all relevant missions.

The windward side is assumed to be protected by a combination of US AETB-12 TUFI and CMC, with variable insulation thickness beneath. For the upper surface, TABI or AFRSI is employed, similar to the configuration used on the Space Shuttle as well as the metallic titanium top layers on major parts of the wing. The total mass of the hot thermal protection is estimated slightly above 14.5 tons.

A small area at the nose and leading edges including the fin needs active cooling [10, 11] and is labeled "Not Defined" in Fig. 13. This actively cooled section is not considered in the passive TPS sizing and has been an important element of the SpaceLiner concept since the early days of the vision [3]. Different cooling ideas have been evaluated and transpiration methods were tested in wind tunnel conditions [9, 10]. An overview on the active cooling types considered for the SpaceLiner is found in Ref. [11]. The cooling hardware including fluid storage tanks and pipes was estimated for SpaceLiner 7 at about 1415 kg [11] and this mass has been preliminarily considered for SpaceLiner 8. A dedicated SLP-8-mission redesign of the active cooling will be part of future design iterations.

3.4.3 Vehicle dry and lift-off mass

Total dry weight of the upper stage is estimated slightly below 109 Mg (Table 3). For the passenger stage, the total fluid and propellant mass of 233.5 Mg includes all liquid ascent, residual, and RCS propellants, solid propellants of separation motors and the water needed for the active leading-edge cooling (still based on the SpaceLiner 7 reference mission [11, 12]). The stages' MECO mass is approximately 134.3 Mg. The SpaceLiner 8's GLOW reaches about 1845 Mg below that of the Space Shuttle STS of more than 2000 Mg.

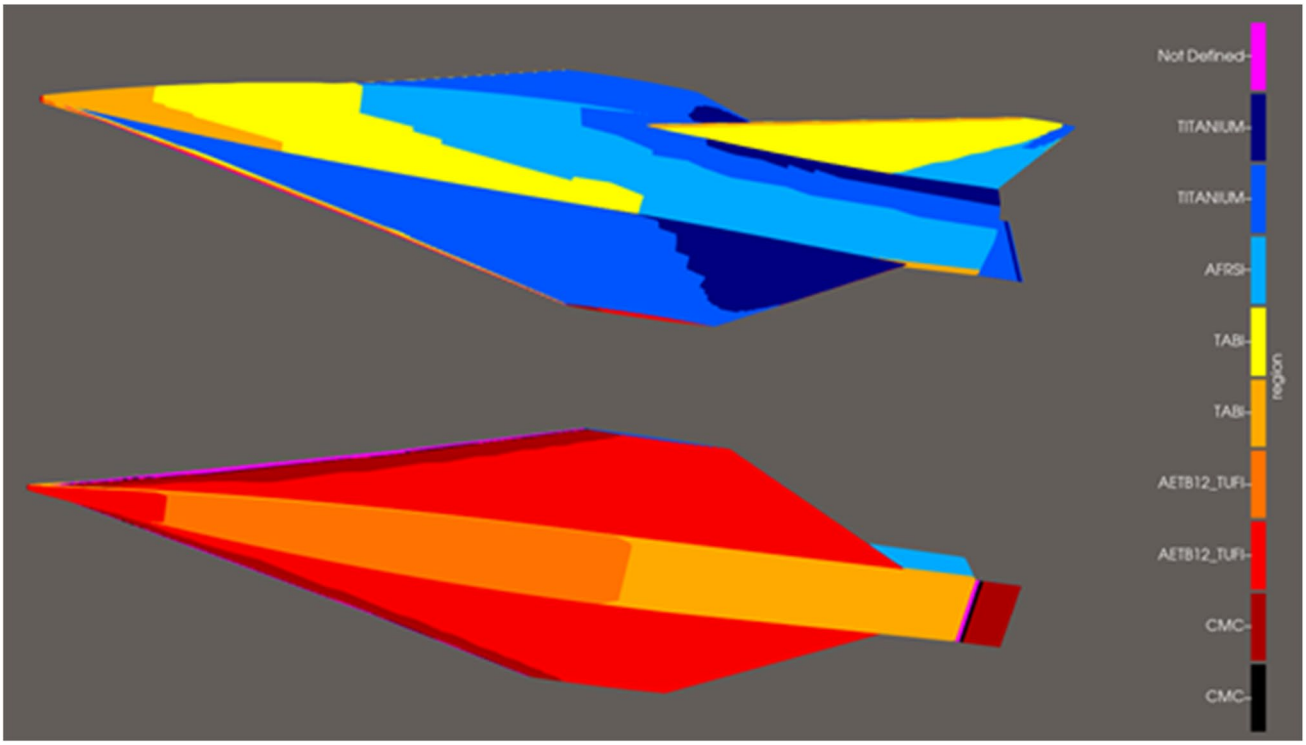

Fig. 13 Preliminary distribution of TPS-types on SLP8 variant O40-0042 in views of the top and bottom sides

Table 3 Mass data of SpaceLiner 8 passenger stage (SLP8 variant O40-0042)

Structure [Mg]	Propulsion [Mg]	Subsystems including cabin [Mg]	TPS [Mg]	Total dry [Mg]	Total fluid and propellant loading [Mg]	GLOW incl. passengers and cargo [Mg]
44.1	11.7	34.3	18.6	108.7	233.5	348.5

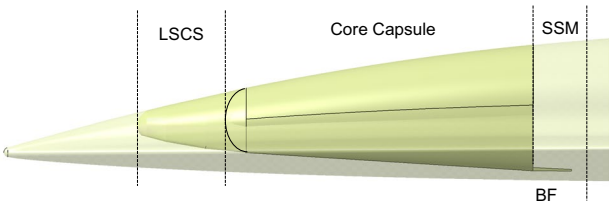

Fig. 14 Potential SLP8 capsule integration concept

3.5 Challenges in defining SLC8 rescue capsule

The functionality of the SpaceLiner 7 capsule design and its stage integration including its shortcomings have already been discussed in Sect. 2.4. As a first measure, the "Type C" integration (schematically shown in Refs. [19, 20]) is selected as a baseline which should allow a simplified and faster separation process simply in the forward direction (Fig. 14). Further, the architecture of SLC8 is split in three sections which should be easily separable.

In a first approach, the core capsule segment is mostly similar to the previous SLC7; however, it is slightly shortened by about 1.5 m. The front pressure dome is the most forward point but no longer includes the ablative TPS on the blunt nose. Instead, a conical nose section (called LSCS) reaches about 3.7 m to the nose and will be protected by TPS. The Liquid Separation and Control System (LSCS) comprises bi-propellant separation motors and the RCS of the stage. The new liquid separation motor is pulling the capsule in case of extreme emergencies and would reduce the number of solid separation motors at the aft end of the capsule from five to four. The LSCS tank system should feed both RCS and separation motors and as this propellant is used in the nominal mission for attitude control and liquid separation motors having a better Isp than solids, a mass saving is expected. With the RCS moved forward, the aft end of the core capsule could be shortened by roughly 1 m.

Behind the capsule, the Solid Separation Motor (SSM) section is placed, still containing four of the previously five solid motors shown in Refs. [19, 20]. However, the SSM is no longer directly connected with the SLC but serves structurally more the role of an interstage. This new connection should bring safety improvements as the solid motors usually remain connected with the SLP stage and only in case of extreme emergency push the SLC out of the danger zone. After a couple of seconds of SLC flight, the exact time will be derived from dynamic simulations. The SSM should be separated from the core capsule. After the potential reentry and most likely before parachute deployment, the LSCS will also be separated to simplify the landing of the capsule.

One critical design point of the current capsule design is the pitch instability which was observed during multi-body dynamics simulations of the separation process [19, 20]. The cabin needs to make an emergency separation at any point in the flight and move itself into a stable flight configuration to fly a reentry trajectory until parachute release. Having a broad stable flight corridor through the whole Mach range is critical for this safety aspect. After initial investigations with small inflatable wings [32] proved unsuccessful in stabilizing the vehicle, an aerodynamic shape optimization study analyzing various rigid wing options was performed [37]. Five different wing design options were investigated:

1. Fixed wings with flaps
2. Fixed wing with flaps and canards in front
3. Rotatable wing around spar (y-axis)
4. Rotatable wing around the joint at the root (x-axis)
5. Rotatable wing in front and back around joint at root (x-axis)

A multi-objective optimization is utilized based on the same evolutionary algorithms applied in the point-to-point trajectory optimizations of Sect. 3.6 to vary capsule wing design parameters like its chord lengths, sweep angle and wing span. The target of the optimization is to find a wing that has the lowest possible added mass and lowest wing area while at the same time maximizing the static pitch stability in the form of a flyable corridor. During the optimization, the algorithm first analyzes the wing's geometry, mass and its impact on the system mass budget, and then the aerodynamics including pitch stability as well as the size of the flight corridor where the vehicle is statically stable.

An exemplary flight corridor is shown in Fig. 15 for the hypersonic range. The stable flight corridor is framed in red with all other points being either trimmable but not stable or neither trimmable nor stable. The target of the optimization has been to increase the number of 'local stable flight corridors' (LSFC) for which an example is shown in a green frame in the figure. If four adjacent AoA and Mach points are all stable, it is assumed that the separated capsule can move through the speed and AoA regime in a stable fashion and, hence, the area is termed 'LSFC'.

On the left of Fig. 16, the Pareto front of wing shape solutions for a fixed-wing design with flaps is shown over all three optimization objectives. The most interesting configuration identified from this Pareto front is framed in red and its modeled shape is displayed on the right-hand side

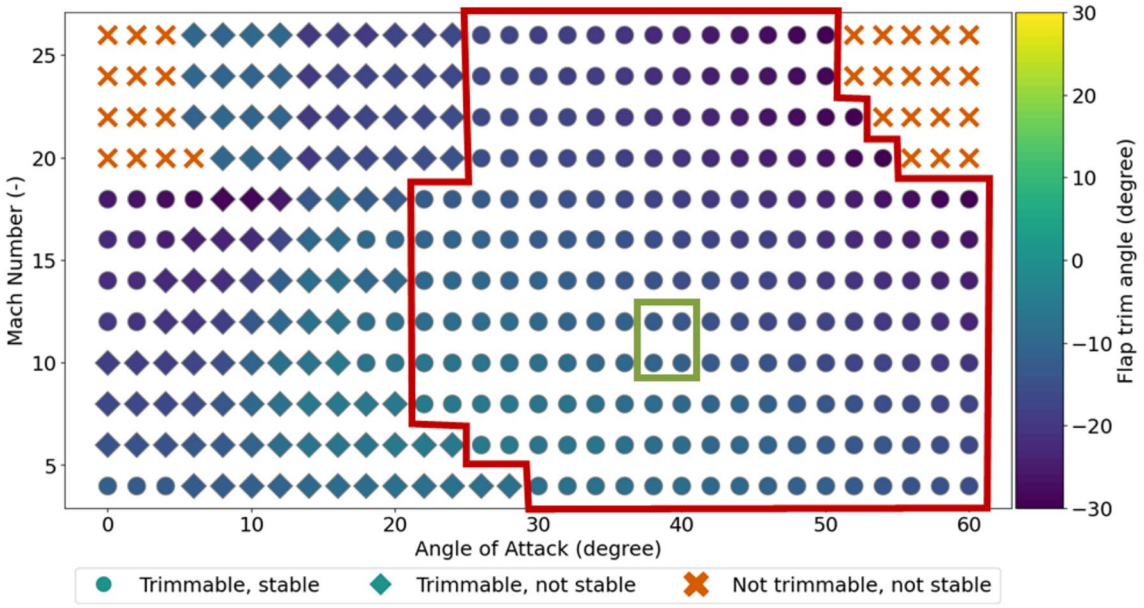

Fig. 15 Typical stability diagram of the SLC8 candidate in the hypersonic range with the flyable corridor (red frame) and an exemplary local stable flight corridor (green frame) marked

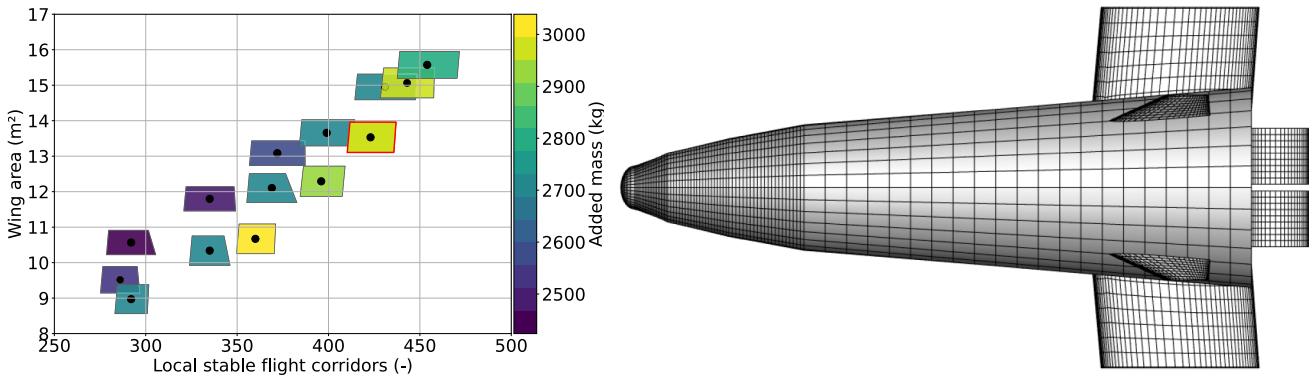

Fig. 16 Left: Pareto front with the wing as marker shape, right: feasible SLC8 configuration including the wing with flaps

of Fig. 16 as a simple aerodynamic grid. The wing is about 4.5 m long and has a half-span of 3.0 m. The sweep angle is 5 degrees and the wing has a maximum relative thickness of 15 percent. The flap takes up about a third of the wing length at a width of 1.6 m. Adding such a wing to the vehicle is expected to increase about 3 tons of mass to the capsule, which is about 8 percent of the original capsule. Out of these 3 tons, 2.6 tons are wing mass and 0.4 tons are resultant propulsion mass that need to be added to ensure the same emergency escape capabilities as with the SLC7.

The same optimization was performed for other wing design options. The obtained geometries can be seen in Fig. 17.

A major critical point is the fact that the systematic assessment of promising capsule configurations has been purely based on static analyses. The separation process itself is highly dynamic and the involved vehicles or components are never in a steady condition during this maneuver. A more sophisticated analysis would be significantly more computationally expensive, the more if flow interference between several potentially tumbling bodies is to be taken into account. On the other hand, the widths of corridors which are required to be flyable in a controlled and stable way might be reduced and, thus, finding solutions could become easier.

The preliminary systematic study simply using fast engineering methods demonstrates that the wing size required for the current capsule design to become longitudinally stable is quite significant. As the capsule is to be smoothly integrated into the SpaceLiner passenger stage's outer mold line, any detailed design on how to install the small capsule auxiliary wing onto the SLP8's main wing will require substantial engineering effort. The integration must not negatively impact the nominal airflow and not create any hot spots on the surface due to the hypersonic flow, but must still ensure a flawless emergency separation. Alternative shapes of the capsule itself or its deployable aerodynamic control should be investigated in the future. Not only should the robustness in pitch trim be assessed, but also the ability to distance the capsule from the danger zone as quickly as possible, whereby the additional mass must be severely limited.

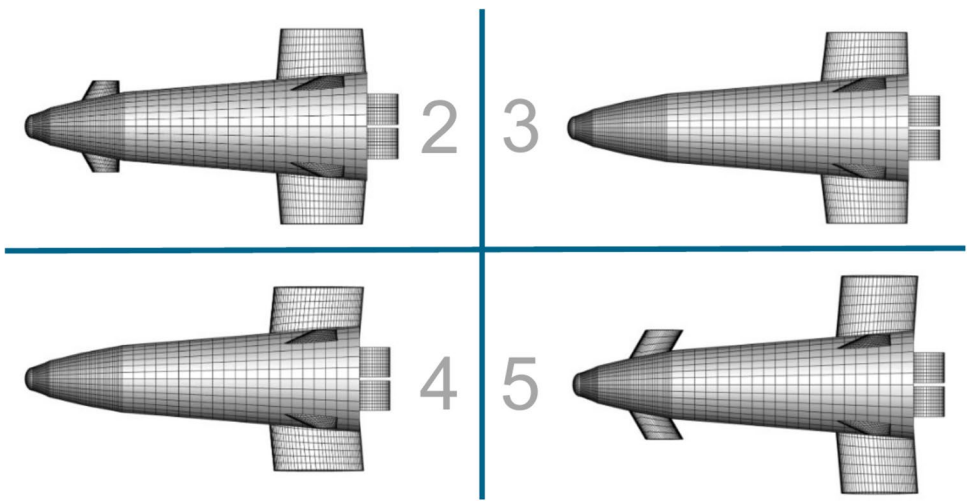

Fig. 17 Overview of alternative SLC8 configuration options 2–5 including wings and flaps

3.6 Intercontinental trajectory options

The SpaceLiner 8 (SL8) passenger stage design enables flying distinctly different trajectories compared to the previous generation SpaceLiner 7 (SL7) [19, 36]. Instead of purely using the high lift-to-drag ratio in the higher atmosphere for a gliding trajectory, in certain cases, the SL8 accelerates outside of the atmosphere to fly a high arc and then re-enter to continue on a gliding flightpath. These flightpaths shall reduce the overall noise disturbance on the general population created from the sonic boom.

This capability is empowered by the smaller wing, with which the vehicle can be trimmed to higher angles of attack of 40 degrees instead of just 20 degrees. Nevertheless, the smaller wing size still has a sufficiently high lift-to-drag ratio to fly long-distance glides in the high atmosphere (Fig. 10), although with a steeper flight-path angle.

To validate the reduction in noise disturbance, the differences between several SL7 and SL8 Earth point-to-point trajectories were analyzed [40]. These trajectories are optimized between the launch and landing sites by using evolutionary algorithms (NSGA-III) to minimize the peak heat flux (and thereby the thermal loads on the vehicle), and the overall overflown population. A global population density database is used to evaluate the population along the trajectory. Because the sonic booms can travel laterally up to about 200 km, the database is adapted to show the worst-case value in a radius of 200 km. Consequently, the optimizer keeps its ground tracks sufficiently far away from population centers, especially at coastlines. Three trajectories are used for the comparison SL7 vs. SL8: Scotland–Australia and vice versa being the acting reference cases for the SpaceLiner, and a new destination from Florida, US to India.

Analyzing the general trajectory characteristics of all three (see Fig. 18), there are distinct differences between SL7 and SL8. First, the SL8 accelerates to higher velocities and higher altitudes. It generally has a higher altitude for the same velocity, which also leads to a reduction in the peak heat flux. Second, as predicted, the SL8 flies outside of the atmosphere to 'jump' over certain populated areas. This is particularly beneficial for trajectories with densely populated regions in the first 5000–10,000 km like with the Australia–Scotland and Florida–India routes (see Fig. 19).

Finally, however, the SL8's lower lift-to-drag ratio in the trimmed state leads to a steeper flight-path angle within the atmosphere which also correlates with a higher sonic boom

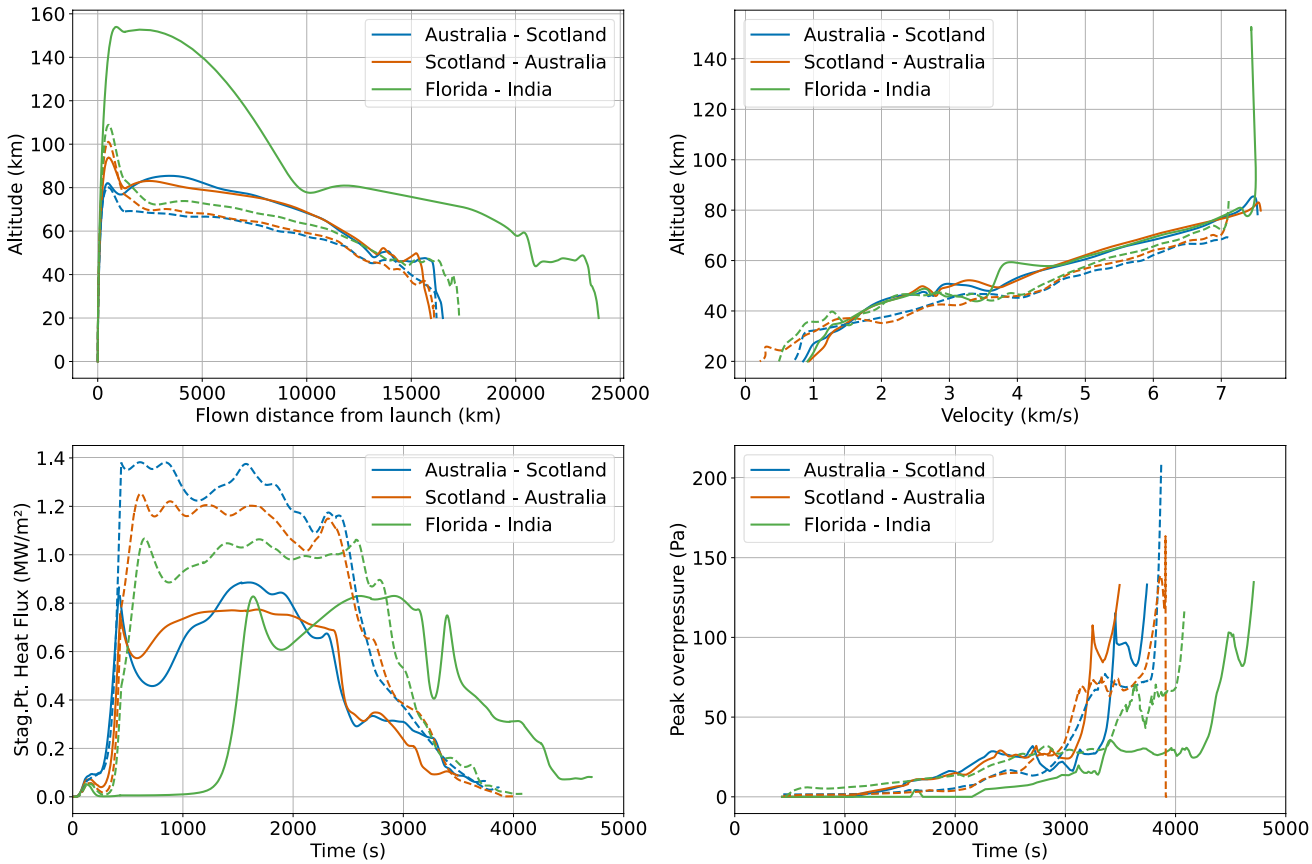

Fig. 18 Overview of the flight profiles between SpaceLiner 8 (solid lines) and SpaceLiner 7 (dashed lines)

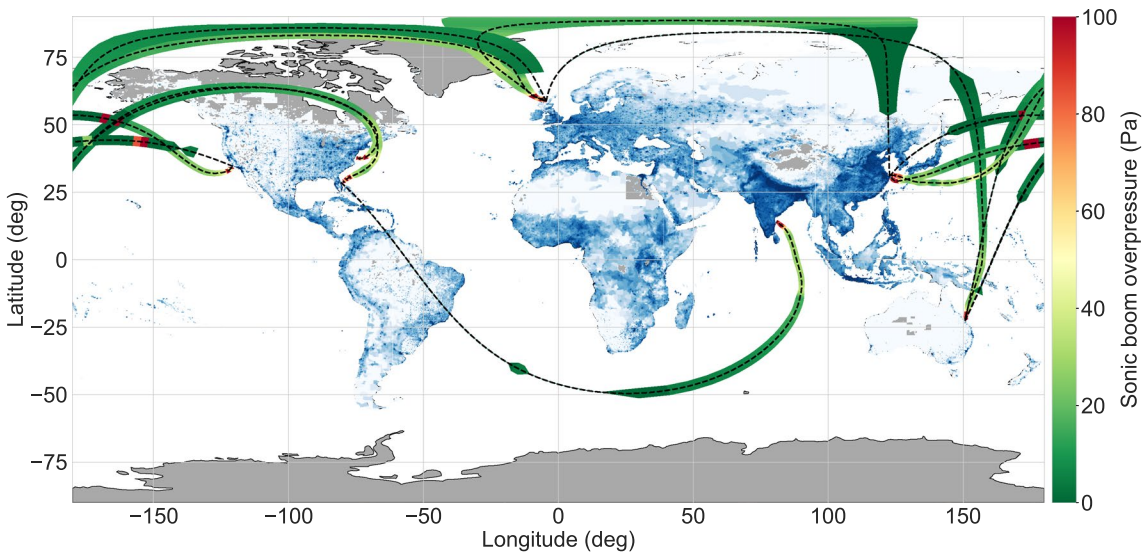

Fig. 19 World map with sonic boom overpressure on ground tracks of investigated SpaceLiner 8 routes

overpressure in this phase. While the SL8 does not create any sonic boom during the exoatmospheric flight, it pays the price with a potentially increased disturbance in a later mission phase [36].

Beyond the three missions used for the SL7–SL8 comparison, six more point-to-point routes were optimized for the SpaceLiner 8 vehicle. These trajectories including their sonic boom carpet can be seen in a world map in Fig. 19.

Generally, this route network avoids populated areas as much as possible by having the vehicle skip over populated areas in the first 5000–10,000 km, and fly predominantly over the oceans and the polar regions. The flight from Florida, US to India is especially remarkable as it flies to over 150 km altitude to completely skip over the Caribbean and South America. Additionally, the flight from Shanghai to California, US does not create any sonic boom over Korea and Japan, which was not possible with the SpaceLiner 7 [36].

Figure 20 shows the overall overflown population for each route and the respective share that is expected to be disturbed based on historic population surveys. Apart from the remarkable case of Florida–India, where the number of overflown people is zero, the number varies between 60,000 and 1.5 million. In comparison, the number of disturbed people according to the ANSI curve (compare, e.g., Ref. [36]) is quite low between a few hundred and less than 100,000 people (see Fig. 21). Most of the disturbance is

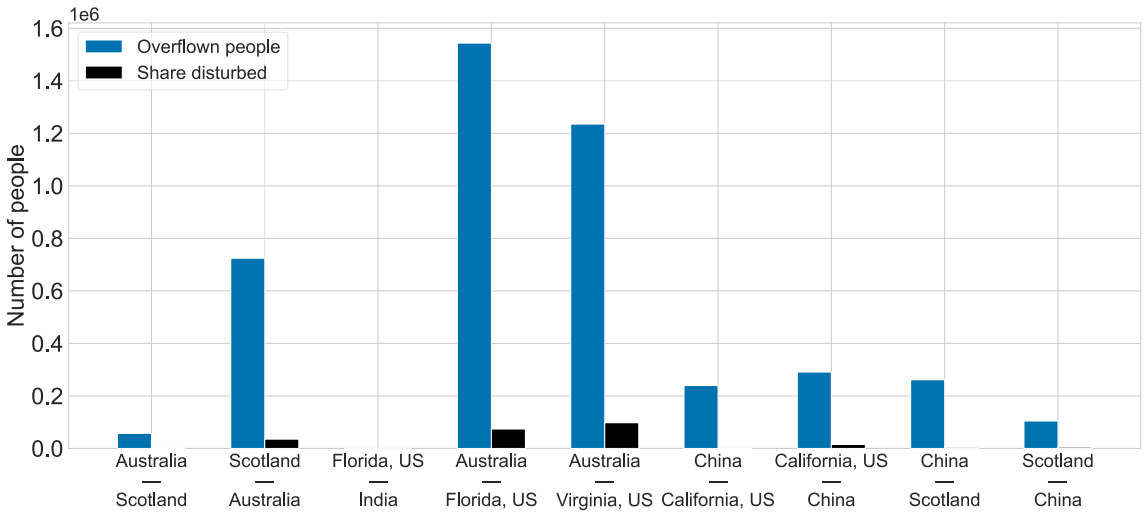

Fig. 20 Overflown people and shared disturbed for investigated SpaceLiner 8 routes

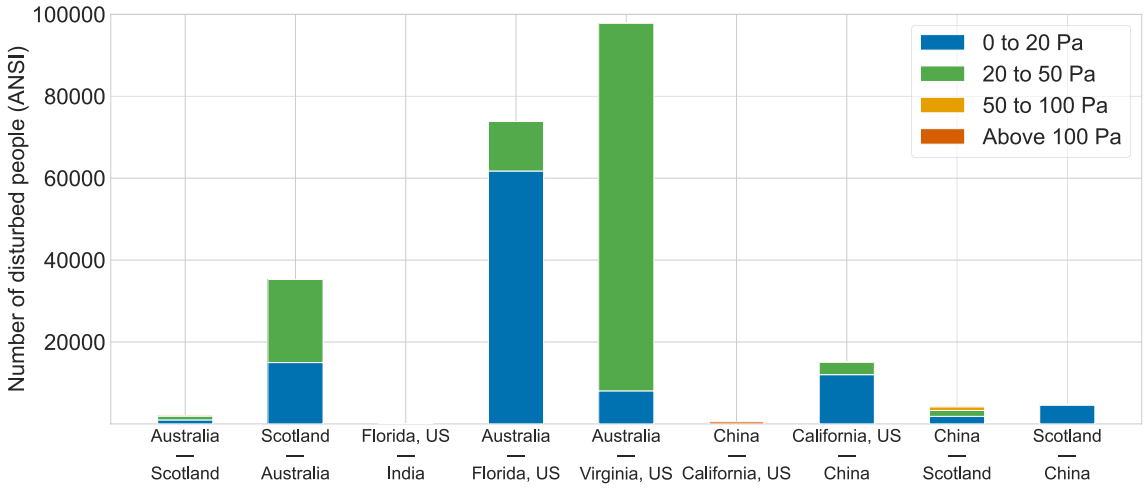

Fig. 21 Detailed analysis of the disturbed population with respect to the overpressure for the investigated SpaceLiner 8 routes

created by sonic booms below 50 Pa which is less than half of what the Concorde caused on the ground.

Another relevant factor for the future evolution of the SL8 design is the actual propellant consumption on the different routes. While the maximum amount of propellant driven by available tank volume defines the achievable flight distance, most routes are shorter than that. Within the performed optimizations, the SL8 booster stage is always assumed as fully fueled and the SLP8's propellant loading is always adjusted exactly for the mission. Thus, in most cases, the passenger stage takes off without full tanks. Table 4 shows an overview of how much the actual burn time and propellant mass are below the maximum for each investigated point-to-point trajectory. Additionally, the used propellant, and percentage of the maximum nominal ascent propellant (214.2 t), within the SLP tanks is shown. Even for the most demanding missions, the current SLP8 variant O40-0042 has propellant volume for a few seconds of remaining burn time. The O40-0042 in general seems to be well sized providing potential performance reserves for other even more demanding point-to-point destinations.

Another interesting aspect to be investigated in the future for cases with substantial propellant volume margin is the option of briefly reigniting the main rocket engines during the gliding phase to sufficiently increase the altitude over populated areas in the latter parts of the flight. This might further reduce the sonic boom overpressure and thus population disturbance for flights like Scotland–Australia for which this annoyance is not completely avoidable with a single engine burn for acceleration and subsequent pure gliding.

Table 4 Overview of required SLP8 O40-0042 propellant mass for investigated SpaceLiner 8 routes

Route	Burn time below maximum	SLP8 used nominal propellant mass	Share of maximum propellant mass
Australia–Scotland	15.09 s	199.8 t	93.3%
Scotland–Australia	5.38 s	209.1 t	97.6%
Florida–India	4.55 s	209.9 t	98.0%
Australia–Florida, US	20.11 s	195.0 t	91.0%
Australia–Virginia, US	31.63 s	184.0 t	85.9%
China–California, US	51.43 s	165.1 t	77.1%
California, US–China	10.29 s	204.4 t	95.4%
China–Scotland	30.65 s	184.9 t	86.3%
Scotland–China	48.72 s	167.7 t	78.3%

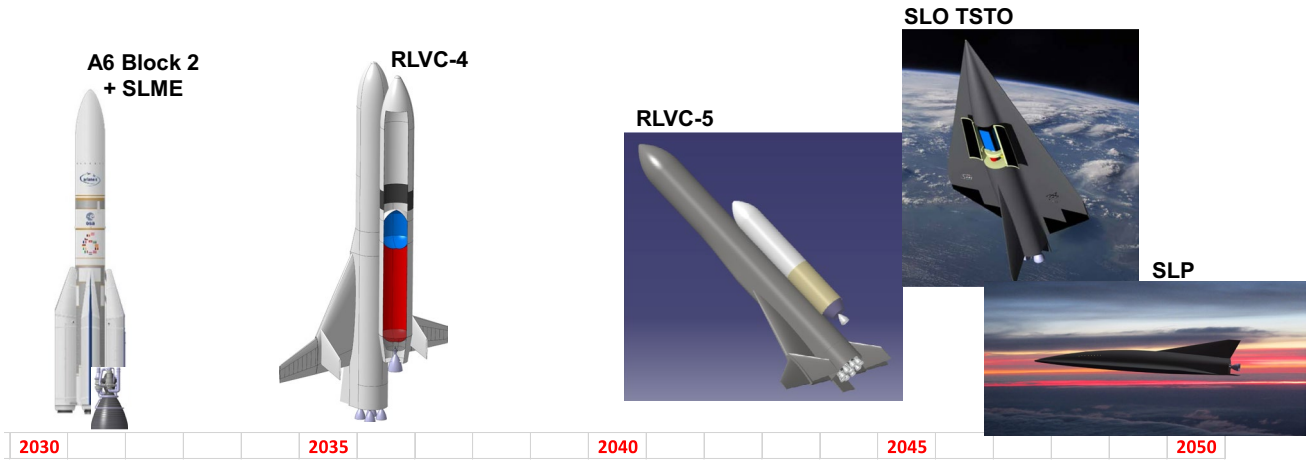

Fig. 22 Roadmap to SpaceLiner in the next 25 years with potential heavy-lift launcher precursors

4 Development roadmap and cost assessments

4.1 Development roadmap including heavy cargo launchers as precursors

Recently, a potential roadmap for a European heavy-lift launcher has been evaluated by DLR [38]. Many elements of the SpaceLiner like SLME or SLB are included as building blocks of such heavy-lift cargo transportation systems. This approach would allow maturing technologies in operations before a high-speed human transport is realized. Such precursors to the SpaceLiner are shown in Fig. 22 in the time scale for the next 25 years which is derived from a more extensive European roadmap for heavy-lift launchers [38].

In fully expendable mode, the A6 performance could approach 30 tons to LEO relatively soon in the early 2030s with the SLME integrated in the A6 core stage. An engine such as the SLME could be matured first in expendable operations before being attached to reusable first stages. Even if the engine might seem oversized for its initial application, the elevated thrust-level in the 2200 kN class will pay off in all future heavy-lift launchers and will be needed by the SpaceLiner. Partially reusable systems might be realized with the cryogenic RLVC-4 and -5 starting from the second half of the 2030s, potentially achieving after 2040 significant payload mass of up to 80 t [38]. Following a sober assessment, a fully reusable TSTO bringing more than 20 tons to LEO as with the SLO is not to be expected before the end of the 2040s.

A semi-reusable option as RLVC-5 carrying heavy payloads and the same or a similar RLV-booster accelerating also the fully reusable upper stage of the SpaceLiner TSTO with missions of lower demand could turn out to be attractive in honing the SpaceLiner design in operations.

4.2 Updated preliminary SpaceLiner cost and funding assessment

From an economic perspective and building on the results of earlier work (see Ref. [41], short summary in Ref. [12]) an updated framework incorporates refined price forecasting and recalibrated cost estimation. Research, Development, Test and Evaluation (RDTE) expenditures are projected at €39–42 billion (e.c. 2025), while Theoretical First Unit (TFU) costs range between €1 and 2.5 billion (e.c. 2025), with an average unit production cost per complete stack decreasing to €550–750 million (e.c. 2025). These numbers are based on an adjustment of Ref. [41] to the 2025 economic conditions. Digitally integrated design methods and modern manufacturing technology have potential for significant cost saving. These are to be leveraged for an attractive business case (see earlier assessment in Ref. [12]). In the near future, SpaceLiner activities will more closely explore this potential.

Direct operating costs per flight are estimated at €4.5–5 million (e.c. 2025) and indirect operating costs add a further €1.5–2.5 million per flight (e.c. 2025). Although results remain preliminary, this cost model for the SpaceLiner identifies the most critical cost drivers for the launch vehicle's development.

From a governance and policy perspective, Europe's ability to foster hypersonic transport initiatives such as the SpaceLiner is somehow weakened by fragmented funding mechanisms and the absence of a coherent, long-term investment strategy. While specific EU-funded programs such as LAPCAT, ATLLAS, FAST20XX, CHATT, HIKARI, FALCon, STRATOFLY or others have advanced relevant technologies, they are not intended to provide the systemic support necessary to cover RDTE and TFU costs, establish regulatory frameworks to operationalize spaceports for

high-speed aviation, or build large-scale industrial plants for next-generation fuels such as liquid hydrogen [42]. By contrast, the United States leverages close coordination between public agencies and large private capital ventures where state contracts and regulatory acceleration sustain technological progress and market entry. China follows a similar path through state-backed programs that integrate academic research with national champions, ensuring vertical alignment between R&D, industrial capacity, and policy roadmaps [43]. Without equivalent pan-European financing mechanisms or strengthened public–private partnerships, Europe risks losing competitiveness in the emerging high-speed aviation ecosystem, with implications not only for commercial viability but also for its long-term aerospace sovereignty [44].

5 Conclusion

The DLR proposed concept SpaceLiner of a reusable winged rocket for very high-speed intercontinental passenger transport is progressing in its conceptual design phase. Research on the vehicle is performed with support from several EC-funded projects with numerous European partners. Assuming advanced but not exotic technologies, a vertically launched rocket-powered two-stage space vehicle is able to transport about 50 passengers over distances of more than 17,000 km in about 1.5 h.

Work is now fully focused on the SpaceLiner 8 definition. A refined modeling of the cryo-tank's reusable insulation on the booster stage (SLB) led to an overall feasible concept but also to an increase in dry weight of the stage. Adding one more SLME on the SLB is the preferred choice for version 8 which limits the overall growth of the SpaceLiner. Sophisticated, automated multidisciplinary analyses helped in finding a compromise out of many design choices in the definition of the upper stage. The promising SLP8 variant O40-0042 with reduced size wing still meets the landing speed constraint and is used for several system trade-offs.

Several intercontinental point-to-point trajectories have been optimized for this variant with the key-objective of minimum disturbance of people on the ground due to sonic boom. Overall, this trajectory study shows that the current SpaceLiner 8 geometry of variant O40-0042 has superior flight dynamic behavior enabling trajectories with significantly reduced (statistical) negative population response. Additionally, the SL8 has a substantially lower peak heat flux as well as an overall integrated heat load which reduces the requirements on the thermal protection system.

The passenger rescue capsule, designed to be used in cases of extreme emergencies, is to be also improved which is addressed in parallel with the SpaceLiner 8 redefinition. The preliminary integration concept of SLC8 is maintained with systematic variation of aerodynamic control and stability devices and its geometric properties. Some aerodynamic configurations are identified which sufficiently fulfill the requirements of stability and trimmability in the broad flight regime. However, significant challenges remain in the definition of the final configuration as the integration of small wings will be difficult, and related mechanisms and structure are heavy. Further modifications with potentially more radical adjustments may be required in the future which should be analyzed also by dynamic simulations.

Finally, a technical development roadmap with precursor applications of RLV-stages is presented and the cost and funding perspective is discussed with updated data.

The SpaceLiner 8 definition is not yet completed but a technically and operationally promising approach is identified and major steps forward are evident.

Acknowledgements The authors gratefully acknowledge the contributions of Ms. Carola Bauer, Ms. Mona Carlsen, Ms. Elena Casali, Ms. Nicole Garbers, Ms. Carina Ludwig, Ms. Sarah Lipp, Ms. Olga Trivailo, Ms. Cecilia Valluchi, Ms. Natascha Bonidis, Mr. Alexander Kopp, Mr. Arnold van Foreest, Mr. Ryoma Yamashiro, Mr. Sven Stappert, Mr. Mete Bayrak, Mr. Magni Johannsson, Mr. David Gerson, Mr. Jochen Bütünley, Mr. Sven Krummen, Mr. Tobias Schwanekamp, Mr. Sholto Forbes-Spyratos, Mr. Marco Palli, Mr. Jan-René Haferkamp, Mr. David von Rüden, Mr. Tommaso Mauriello, Mr. Vincent Friesen, Mr. Tiago Rebelo and Mr. Theau Deroy to the analyses and preliminary design of the SpaceLiner.

Author contributions MS has written major parts of the paper and is responsible for the SpaceLiner concept investigations since its initial research phase. He also established the development roadmap presented in this paper. SC has performed for this paper the MDAO analyses of the SpaceLiner 8 rescue capsule and has run the optimizations of the intercontinental point-to-point trajectories. He has prepared these sections in the paper. SS has prepared and validated the TPS-sizing tool and performed the SLP8 TPS preliminary sizing. She has prepared this section in the paper. JW was one of the supervisors of the SLP8 MDAO and has prepared and validated the TPS-sizing tool. LB has been involved in the SLB8 V3 preliminary sizing and has been responsible for major parts of the aerodynamic analyses with focus on OpenFoam CFD. SRD and DGA have jointly worked on the updated preliminary SpaceLiner cost and funding assessment and they have written this section.

Funding Open Access funding enabled and organized by Projekt DEAL.

Data availability No datasets were generated or analyzed during the current study.

Declarations

Conflict of interest The authors declare no competing interests.

References

1. Musk, E.: Making life multi-planetary. New Space (2018). https://doi.org/10.1089/space.2018.29013.emu
2. Sippel, M., Klevanski, J., Steelant, J.: Comparative study on options for high-speed intercontinental passenger transports: air-breathing- vs. rocket-propelled, IAC-05-D2.4.09 (2005)
3. Sippel, M., Klevanski, J., van Foreest, A., Gülhan, A., Esser, B., Kuhn, M.: The SpaceLiner Concept and its Aerothermodynamic Challenges, 1st ARA-Days, Arcachon (2006)
4. Trivailo, O. et.al.: SpaceLiner mission requirements document, SL-MR-SART-00001-1/2, Issue 1, Revision 2, SART TN-005/2016, 11.07.2016
5. Sippel, M., Schwanekamp, T, Trivailo, O, Kopp, A, Bauer, C, Garbers, N.: SpaceLiner technical progress and mission definition. In: AIAA 2015–3582, 20th AIAA international space planes and hypersonic systems and technologies conference, Glasgow (2015)
6. Sippel, M.; Stappert, S.; Bussler, L.; Forbes-Spyratos, S.: Technical progress of multiple-mission reusable launch vehicle SpaceLiner, HiSST 2018–1580839. In: 1st HiSST: international conference on high-speed vehicle science technology, Moscow (2018).
7. Sippel, M., Stappert, S., Koch, A.: Assessment of multiple mission reusable launch vehicles. J. Space Saf. Eng. **6**, 165–180 (2019). https://doi.org/10.1016/j.jsse.2019.09.001
8. Sippel, M., Stappert, S., Bussler, L., Singh, S., Krummen, S.: Ultra-fast passenger transport options enabled by reusable launch vehicles. In: 1st FAR conference, Monopoli, September 30th – October, 3rd 2019
9. Van Foreest, A., Sippel, M., Gülhan, A., Esser, B., Ambrosius, B.A.C., Sudmeijer, K.: Transpiration cooling using liquid water. J. Thermophys. Heat Transfer **23**, 4 (2009)
10. Reimer, Th., Kuhn, M., Gülhan, A., Esser, B., Sippel, M., van Foreest, A.: Transpiration cooling tests of porous CMC in hypersonic flow. In: AIAA2011–2251, 17th international space planes and hypersonic systems and technologies conference (2011)
11. Schwanekamp, T., Mayer, F., Reimer, T., Petkov, I., Tröltzsch, A., Siggel, M.: System studies on active thermal protection of a hypersonic suborbital passenger transport vehicle. In: AIAA aviation conference, AIAA 2014–2372, Atlanta, June 2014
12. Sippel, M., Trivailo, O., Bussler, L., Lipp, S., Kaltenhäuser, S.; Molina, R.: Evolution of the SpaceLiner towards a reusable TSTO-launcher, IAC-16-D2.4.03, September 2016
13. Sippel, M., Bussler, L., Kopp, A., Krummen, S., Valluchi, C., Wilken, J., Prévereaud, Y., Vérant, J.-L., Laroche, E., Sourgen, E., Bonetti, D.: Advanced simulations of reusable hypersonic rocket-powered stages. In: AIAA 2017–2170, 21st AIAA international space planes and hypersonic systems and technologies conference, 6–9 March 2017, Xiamen, China
14. Sippel, M., Dietlein, I., Wilken, J., Pastrikakis, V., Barannik, V., du Toit, T.H.J., Moroz, L System Aspects of European Reusable Staged-Combustion Rocket Engine SLME, Space Propulsion Conference, Glasgow, 20–23 May 2024
15. Sippel, M., Singh, S., Stappert, S.: Progress summary of H2020-project FALCon. In: Aerospace Europe conference 2023 – 10th EUCASS – 9th CEAS, Lausanne July 2023
16. Singh, S., Bussler, L, Bergmann, K., Sippel, M: Mission design and sensitivity analysis for in-air capturing of a winged reusable launch vehicle. In: IAC-23-D2.5.5, 74th international astronautical congress (IAC), Baku, Azerbaijan, 2–6 October 2023,
17. Singh, S.: Relative navigation implementation for the in-air capturing of a winged reusable launch vehicle, HiSST 2024 – 279, 3rd HiSST conference, Busan, April 2024
18. Callsen, S., Wilken, J., Stappert, S., Sippel, M.: Feasible options for point-to-point passenger transport with rocket propelled reusable launch vehicles. Acta Astronaut. **212**, 100–110 (2023). https://doi.org/10.1016/j.actaastro.2023.07.016
19. Sippel, M., Stappert, S., Bayrak, Y.M.; Bussler, L., Callsen, S.: Systematic assessment of SpaceLiner passenger cabin emergency separation using multi-body simulations. In: 2nd HiSST-conference, Bruges, September 2022
20. Sippel, M., Stappert, S., Bayrak, Y.M., Bussler, L.: Systematic assessment of SpaceLiner passenger cabin emergency separation using multi-body simulations. CEAS Space J. (2023). https://doi.org/10.1007/s12567-023-00505-z. (**published online: 02 June 2023**)
21. Krummen, S., Sippel, M.: Effects of the rotational vehicle dynamics on the ascent flight trajectory of the SpaceLiner concept. CEAS Space J. **11**, 161–172 (2019). https://doi.org/10.1007/s12567-018-0223-7
22. Bauer, C., Kopp, A., Schwanekamp, T., Clark, V., Garbers, N.: Passenger capsule for the SpaceLiner, DLRK-paper, Augsburg 2014
23. Valluchi, C., Sippel, M.: Hypersonic morphing for the SpaceLiner cabin escape system. In: 7th European conference for aeronautics and space sciences (EUCASS), Milan 2017
24. Bayrak, Y.M.: Multi-body Simulation of the SpaceLiner cabin rescue system, SART TN-009/2019, October 2019
25. Sippel, M., Callsen, S., Bussler, L.: SpaceLiner system specification document: main propulsion integration, SART TN-006/2024, SL-SS-MPI-SART-00043–1/0, 2024
26. Bussler, L, Sippel, M., von Rüden, D.F.: Reference concept SLB 8 booster, AKIRA report R-2004, SART TN-001/2020, March 2020
27. Herberhold, M., Bussler, L., Sippel, M., Wilken, J.: Comparison of SpaceX's Starship with winged heavy-lift launcher options for Europe. CEAS Space J. (2025). https://doi.org/10.1007/s12567-025-00625-8
28. Sippel, M. et al: Enhancing critical RLV-technologies: testing reusable cryo-tank insulations. In: IAC-19-D2.5.10, 70th international astronautical congress, Washington (2019)
29. Rauh, C.; Reimer, T.; Sippel, M.; Wilken, J.; Liebisch, M.; Hildebrandt, B.: DLR concepts of advanced thermal protection systems for reusable cryogenic propellant tanks. In: 3rd FAR-conference, Arcachon, 18th-22nd May 2025
30. Reimer, T., Rauh, C., Di Martino, G.D., Sippel, M.: Thermal investigation of a purged insulation system for a reusable cryogenic tank. J. Spacecr. Rockets **59**(4), 1205–1213 (2022). https://doi.org/10.2514/1.A35252
31. Sippel, M., Wilken, J., Callsen, S.; Bussler, L.: Towards the next step: SpaceLiner 8 pre-definition. In: IAC-23-D2.4.2, 74th International Astronautical Congress (IAC), Baku, Azerbaijan, 2023
32. Sippel, M., Wilken, J., Bussler, L., Callsen, S., Mauriello, T.: Progress in pre-definition of the SpaceLiner 8 Advanced Hypersonic Transport. In: 3rd international conference on high-speed vehicle science technology (HiSST), April 2024, Busan, Korea
33. Mauriello, T.: Multidisciplinary design analysis & optimization of the SpaceLiner passenger stage, SART TN-014/2023 (2023)
34. Mauriello, T., Wilken, J., Callsen, S., Bussler, L., Sippel, M.: Multidisciplinary design analysis and optimization of the aerodynamic shape of the SpaceLiner passenger stage. Acta Astronaut. (2024). https://doi.org/10.1016/j.actaastro.2024.07.054
35. Mauriello, T., Callsen, S., Bussler, L, Wilken, J., Sippel, M.: Multidisciplinary design assessment of promising aerodynamic shapes

for hypersonic passenger transport. In: IAC-24-D2.4.6, 75th international astronautical congress (IAC), Milan, Italy (2024)
36. Callsen, S., Wilken, J., Sippel, M.: Analysis of sonic boom propagation and population disturbance of hypersonic vehicle trajectories. CEAS Space J. (2025). https://doi.org/10.1007/s12567-024-00583-7. (**Online 19.12.2024**)
37. Callsen, S., Bussler, L., Sippel, M.: Aerodynamic stability and system impact analysis of SpaceLiner passenger and rescue cabin. In: 3rd FAR-conference, Arcachon, France, 18th-22nd May 2025
38. Sippel, M., Dietlein, I., Herberhold, M.; Bergmann, K.; Bussler, L.: Future reusable launcher options for Europe: the heavy class segment. In: 11th European conference for AeroSpace sciences (EUCASS), Rome 30th June–4th July 2025
39. Sippel, M., Callsen, S.; Wilken, J., Bussler, L.; Singh, S.; Mauriello, T.: SpaceLiner 8 definition: relevant aerodynamic and aerothermodynamic issues. In: 3rd FAR-conference, Arcachon, 18th–22nd May 2025
40. Callsen, S., Wilken, J., Sippel, M.: Analysis of flight profile and sonic boom population response of updated aerodynamic configuration for hypersonic passenger transport. In: 11th European conference for AeroSpace sciences (EUCASS), Rome, Italy, 30th June–04th July 2025
41. Trivailo, O.: Innovative cost engineering analyses and methods applied to SpaceLiner—an advanced, hypersonic, suborbital spaceplane case-study, PhD Thesis (2015)
42. European Commission: A hydrogen strategy for a climate-neutral Europe (COM/2020/301 final). Publications Office of the European Union, 2020 https://energy.ec.europa.eu/system/files/2020-07/hydrogen_strategy_0.pdf
43. Daniel: Hypersonic era accelerates: U.S. and China race for supremacy in high-speed aerospace, The Defense Watch, August 26, 2025, https://thedefensewatch.com/aerospace-aviation/hypersonic-era-accelerates-u-s-and-china-race/
44. Rodriguez-Donaire, S., Gil, P., Garcia-Almiñana, D., Crisp, N., Herdrich, G., Roberts, P., Kataria, D., Hanessian, V., Becedas, J., Seminari, S.: Business roadmap for the European Union in the NewSpace ecosystem: a case study for access to space. CEAS Space J. **14**(4), 785–804 (2022). https://doi.org/10.1007/s12567-022-00450-3